Five Years of Solar Observation with PICARD

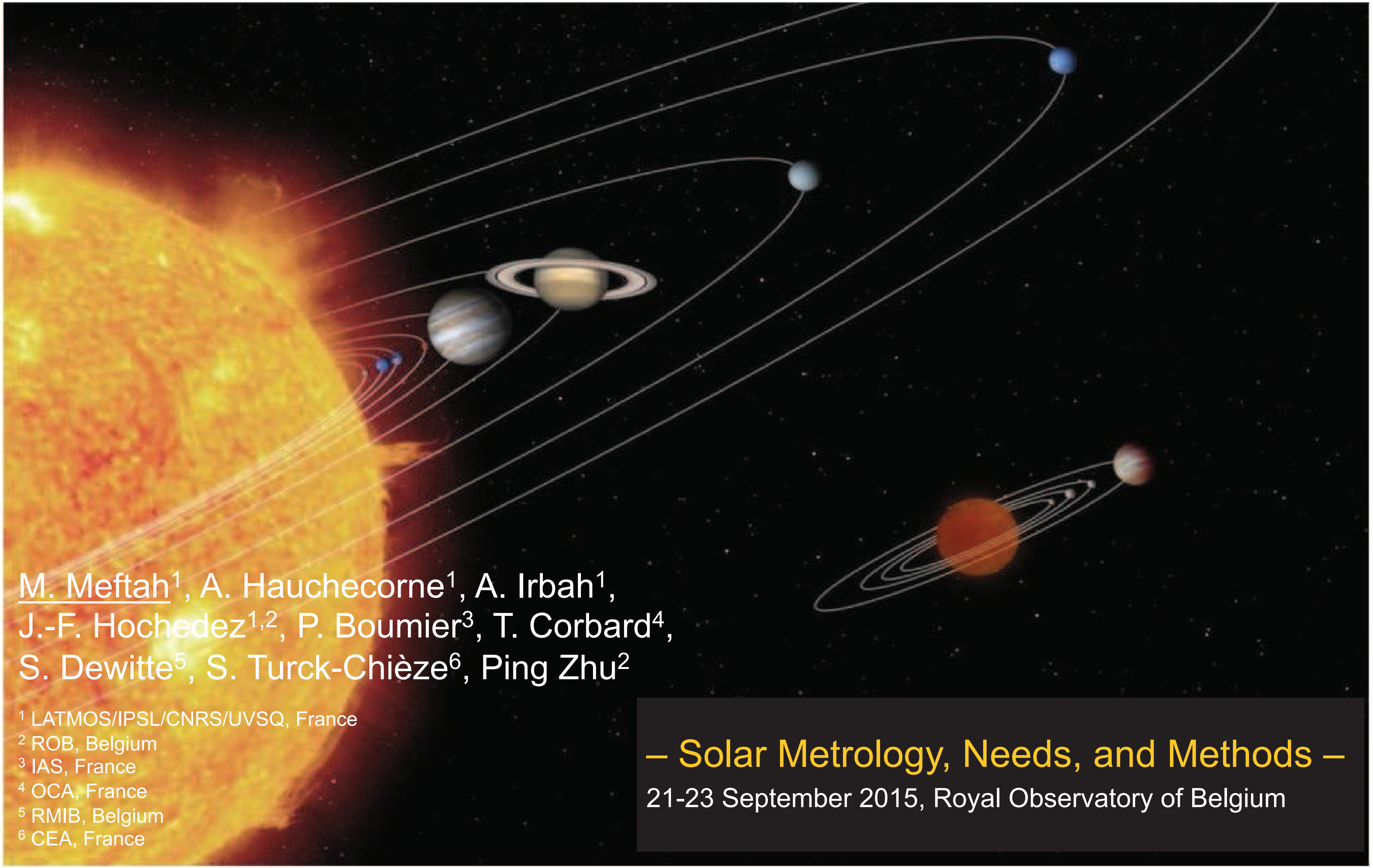

M. Meftah[1], A. Hauchecorne[1], A. Irbah[1], J.-F. Hochedez[1,2], P. Boumier[3], T. Corbard[4], S. Dewitte[5], S. Turck-Chièze[6], Ping Zhu[2]

[1] LATMOS/IPSL/CNRS/UVSQ, France
[2] ROB, Belgium
[3] IAS, France
[4] OCA, France
[5] RMIB, Belgium
[6] CEA, France

– Solar Metrology, Needs, and Methods –

21-23 September 2015, Royal Observatory of Belgium

On solar radius measurements during the rising phase of solar cycle 24

Presentation outline

- The PICARD mission and the scientific objectives
- The payload of the PICARD mission
- PICARD SOL, our ground-based facility
- Scientific results
- Conclusion

1 – The PICARD mission and the scientific objectives (1/5)

PICARD is a scientific mission dedicated to the study of the Sun.

The name of the mission comes from Jean Picard (1620-1682), a pioneer of precise modern astrometry, who observed the sunspots, and measured their rotation velocity and the solar diameter.

The Picard mission expands observations of the global parameters of the Sun in the hope of linking the variability of its total and spectral irradiance to its geometric shape.

PICARD observations are made during the ascending phase and the plateau of solar cycle 24.

Jean Picard (1620-1682)

Five Years of Solar Observation

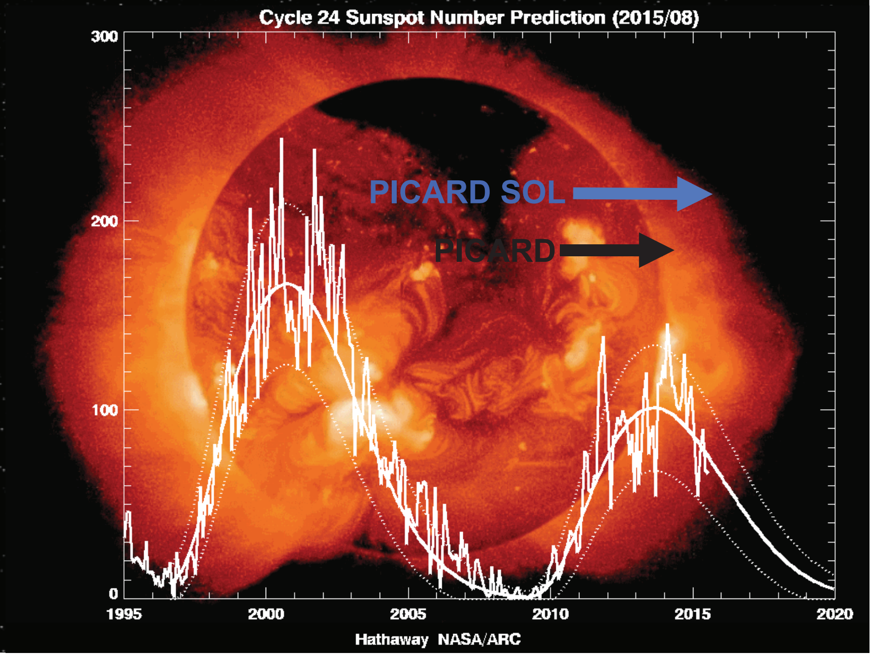

1 – The PICARD mission and the scientific objectives (2/5)

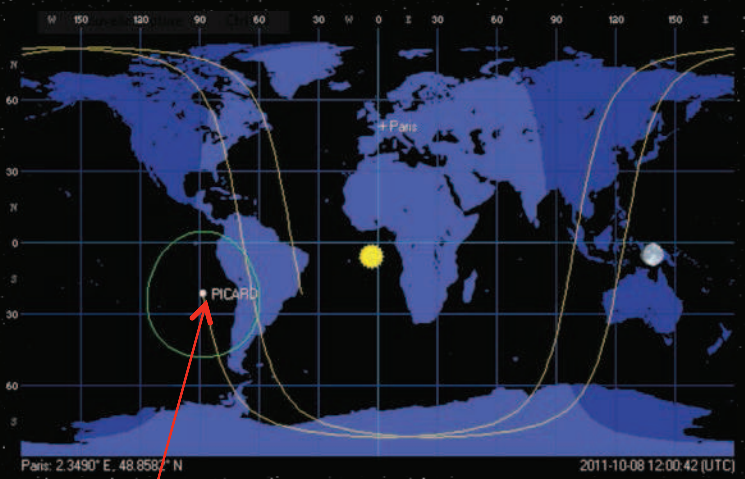

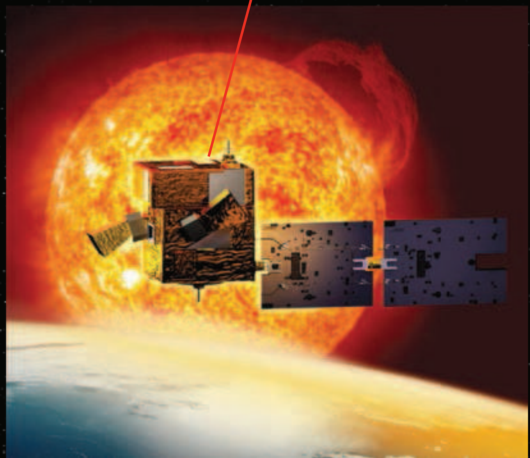

PICARD is a space mission, which was successfully launched on 15 June 2010 into a Sun synchronous dawn-dusk orbit (735 km, Inclination: 98.29°).

PICARD SOL is the ground component of the PICARD mission and is operational since March 2011 (Calern, France) – OCA and LATMOS (CNRS).

1 – The PICARD mission and the scientific objectives (3/5)

PICARD

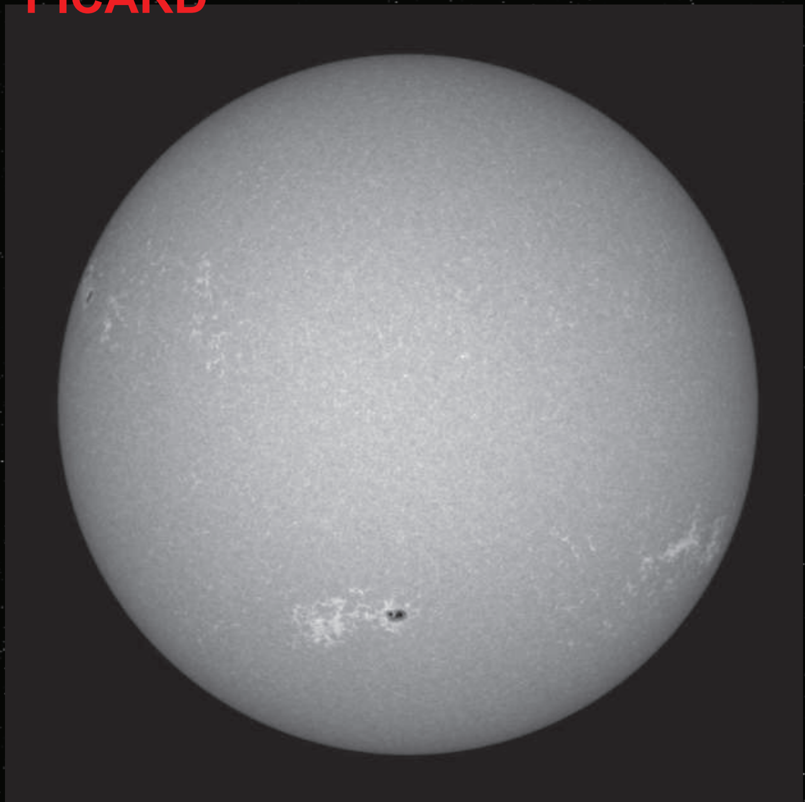

~ 1,300,000 images acquired

PICARD has recorded more than one million solar images from June 2010 to April 2014.

PICARD SOL

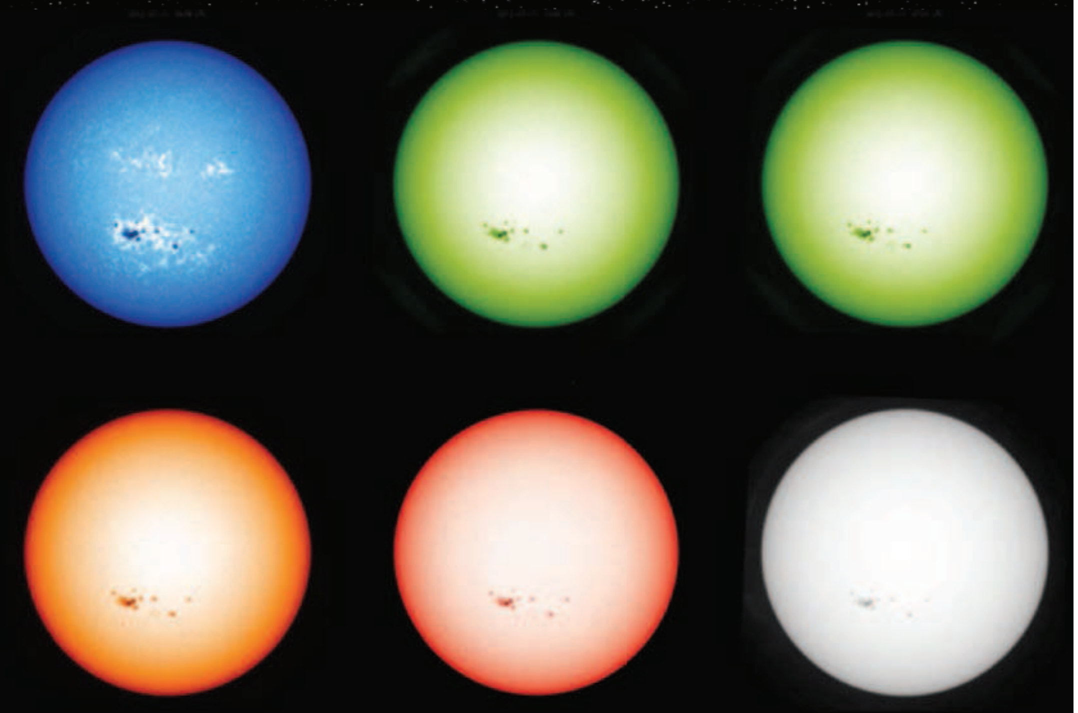

~ 100,000 images acquired

PICARD SOL operates nominally since 2011.

1 – The PICARD mission and the scientific objectives (4/5)

- Solar Astrometry

Measure the diameter and the solar oblateness of the Sun (absolute values) and their changes over time.

- Radiometry and photometry

Measure the total solar irradiance (TSI) in absolute and over time.
Impact on the climate.

Establish the relationship: variation of the solar diameter / change of the TSI (solar parameter W).

Measure the variations of the solar spectral irradiance in the UV (influence on ozone and climate).

- Helioseismology

Observations of low-frequency acoustic oscillations and detection of the p-modes (detailed study of the nuclear core and his dynamics).

1 – The PICARD mission and the scientific objectives (5/5)

<u>Variability of the solar radius, solar oblateness, and magnetic field</u>

Why it varies ? What is the impact on the variability of the spectral irradiance ?

<u>Time variation of the solar radius</u>

– Influence of inner magnetic field ?
– Other influences ?
– Order of magnitudes: measurable or not ?

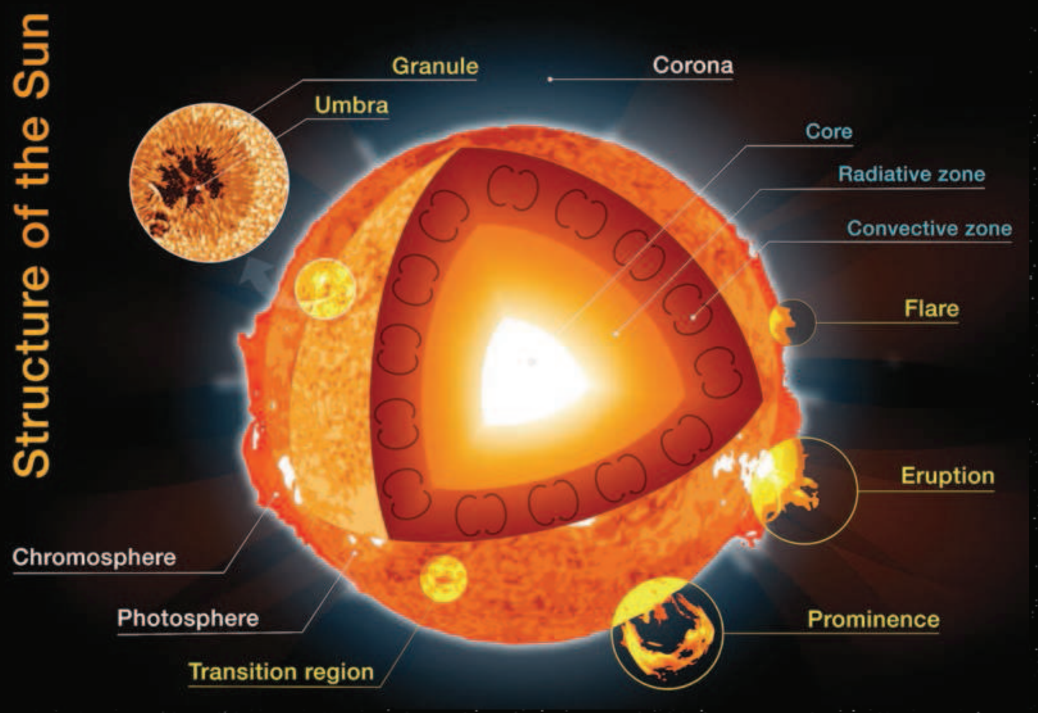

1) The first step is to determine the evolution of the solar radius during the solar cycle 24.

2) Next, we will determine the evolution of the spectral solar irradiance over time.

Presentation outline

- The PICARD mission and the scientific objectives
- The payload of the PICARD mission
- PICARD SOL, our ground-based facility
- Scientific results
- Conclusion

2 – The payload of the PICARD mission (1/5)

PICARD is a microsatellite of 130 kg mass (CNES), dedicated to the study of the Sun.

Main instruments:

- **SODISM** (SOlar Diameter Imager and Surface Mapper) is an imaging telescope
- **SOVAP** (SOlar VAriability PICARD) is a radiometer
- **PREMOS** (PREcision MOnitoring Sensor) is a photometer and radiometer
- **PGCU** is an onboard electronics

Responsibility of the payload (LATMOS)

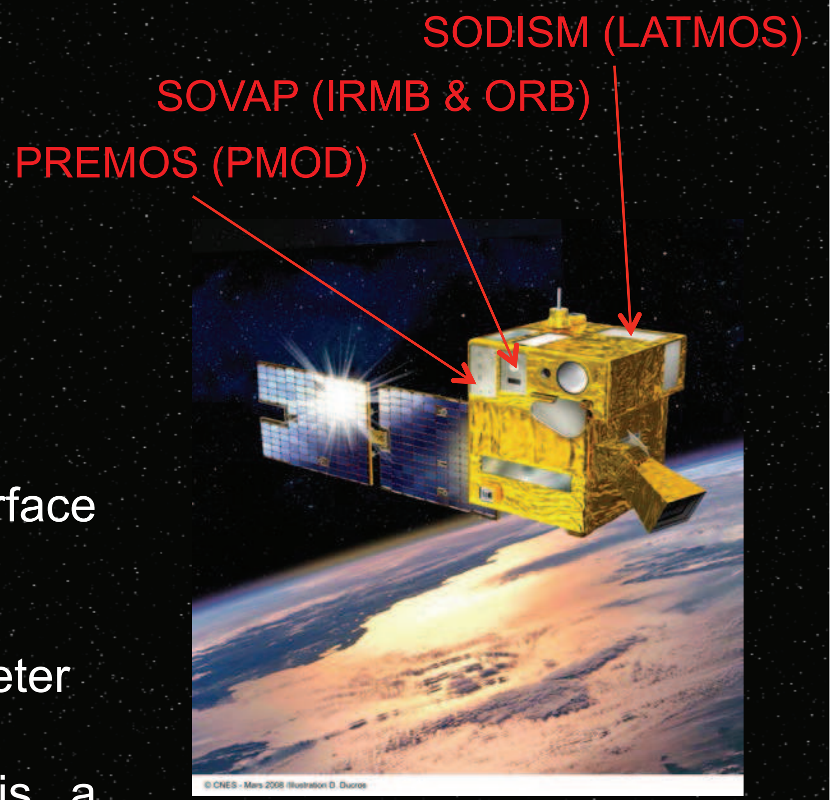

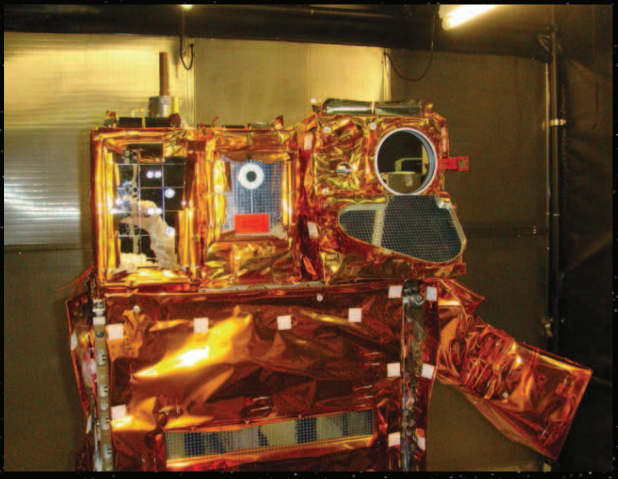

2 – The payload of the PICARD mission (2/5)

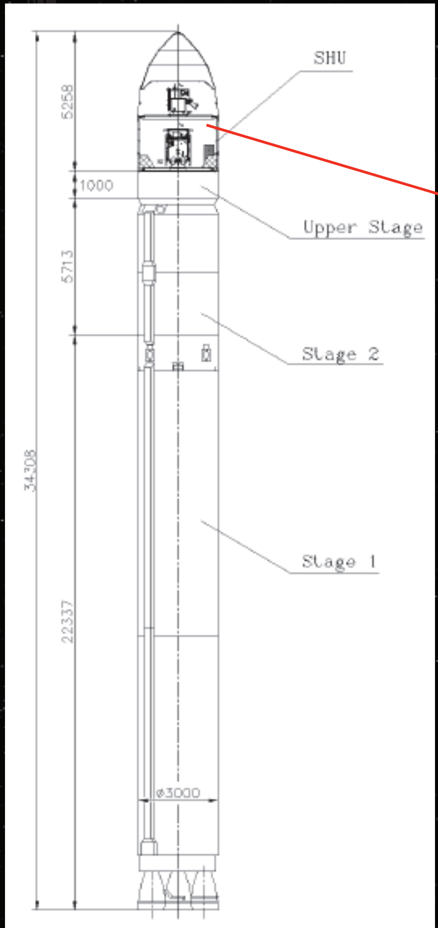

Launch vehicle

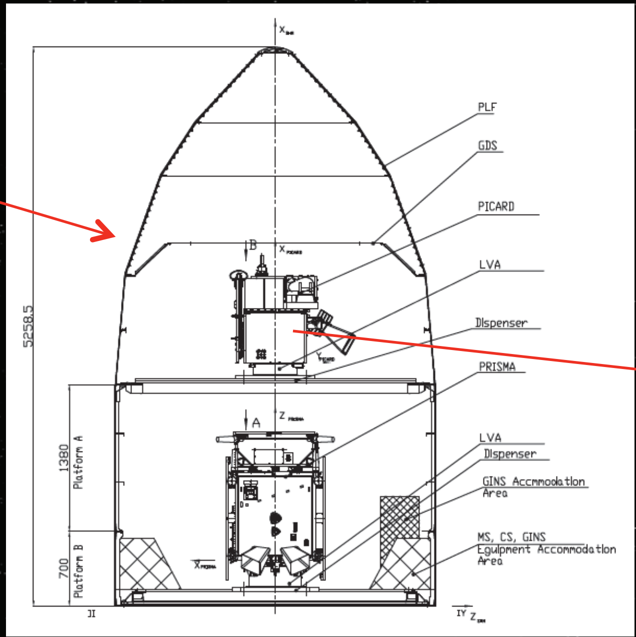

Rocket payload unit general view

Stowed view (launch)

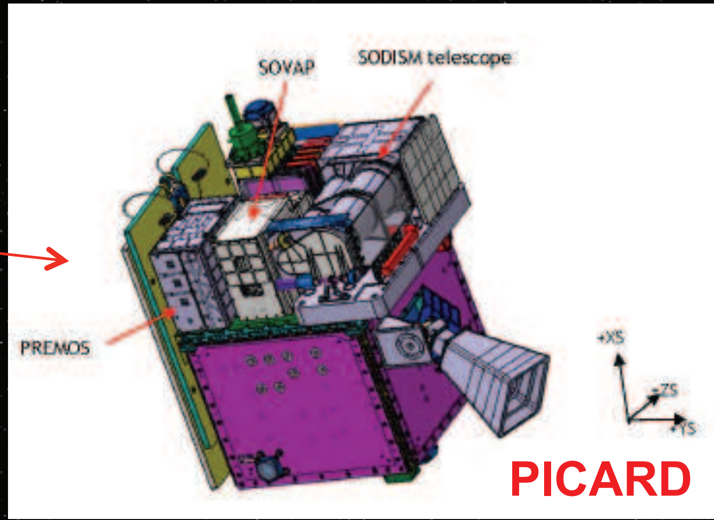

Deployed on orbit

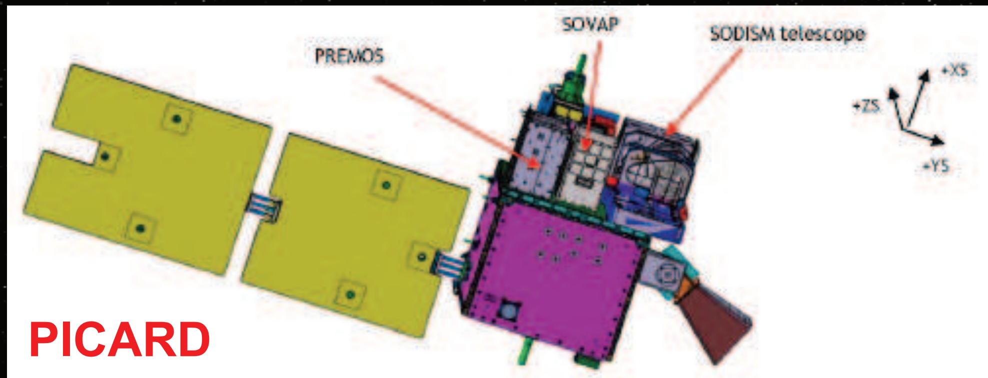

2 – The PICARD/SODISM space instrument (3/5)

SODISM is an 11-cm Ritchey-Chretien imaging telescope developed at CNRS by LATMOS (ex. Service d'Aéronomie, France) associated with a 2Kx2K Charge-Coupled Device (CCD), taking solar images at five wavelengths.

SODISM main characteristics:

- Telescope type: Ritchey Chretien
- Focal length: 2626 mm
- Field of view: 35 arc-minutes
- Angular resolution: 1.06 arc-second
- Dimensions: 300x308x370 mm^3
- Mass: 26.4 kg
- Power: 30.6 W
- Data flow: 2.2 Gbits per day
- One image per minute

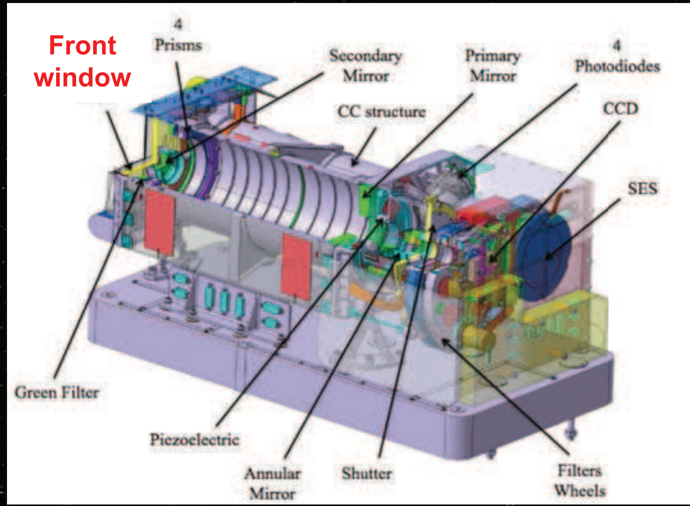

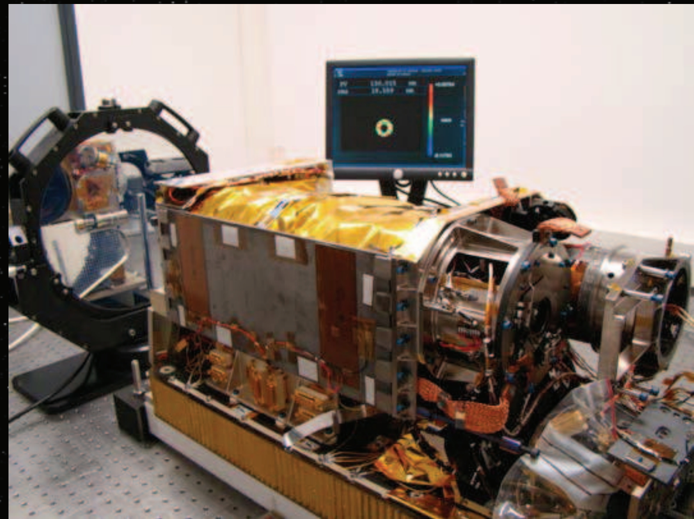

2 – The PICARD/SODISM space instrument (4/5)

SODISM optical path and interferential filters characteristics

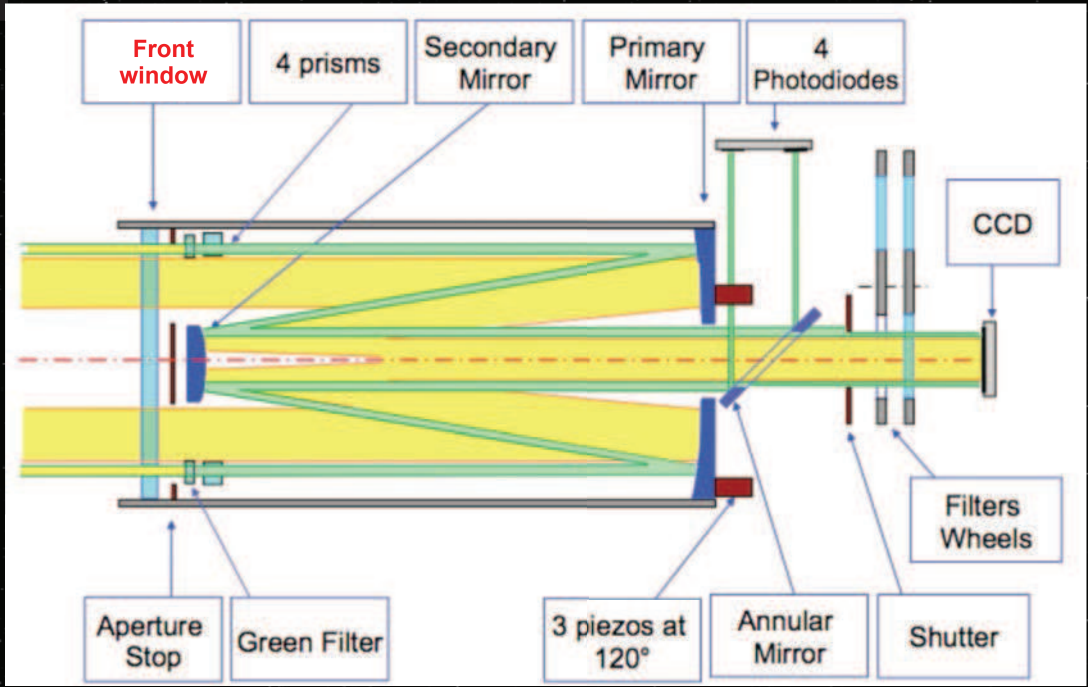

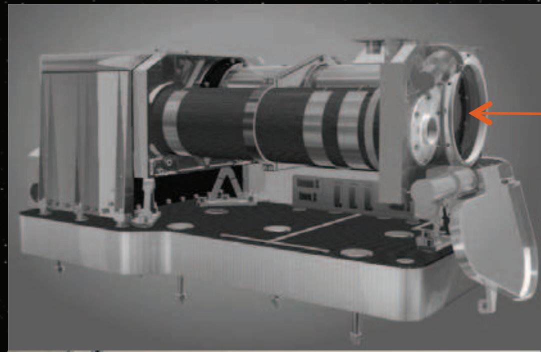

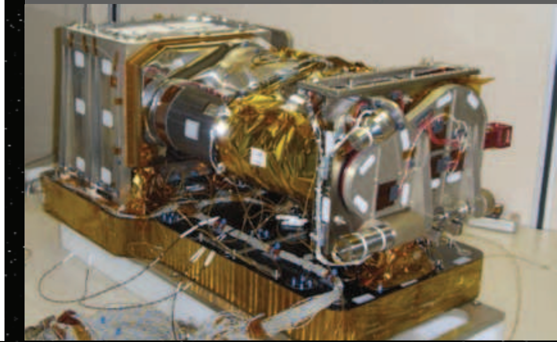

Wavelength λ in nm	Bandwidth Δλ in nm	Function
215.0	7	Sun activity, O3, measurement, diameter
393.37	0.7	Active regions observation
535.7	0.5	Oscillations (helioseismology)
535.7	0.5	Diameter, oscillations (helioseismology)
607.1	0.7	Diameter
782.2	1.6	Diameter

2 – The PICARD/SODISM space instrument (5/5)

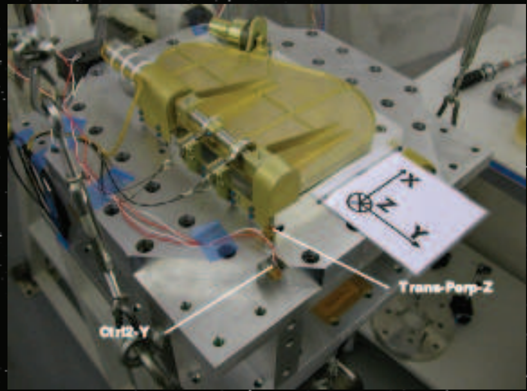

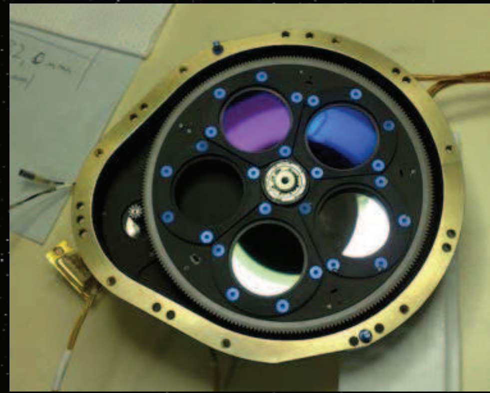

SODISM, an imaging telescope with a lot of mechanisms and many technology

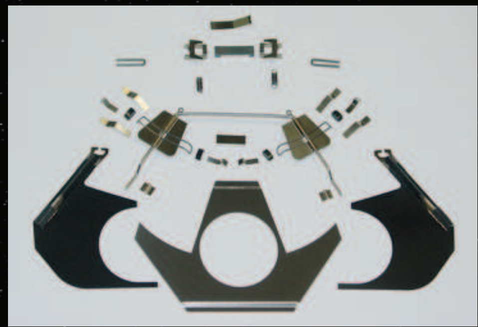

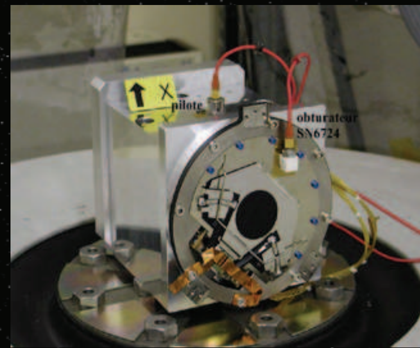

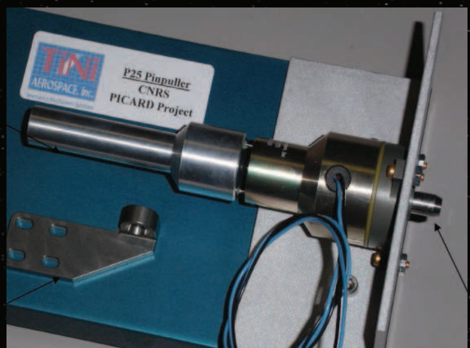

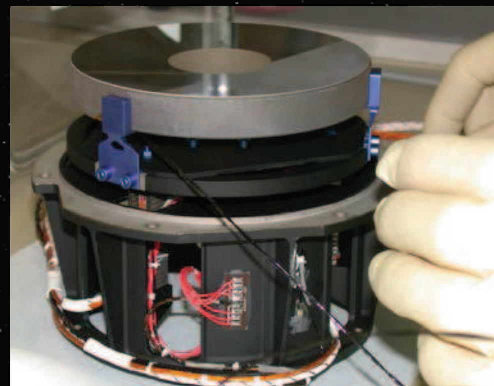

Presentation outline

- The PICARD mission and the scientific objectives
- The PICARD/SODISM space instrument
- PICARD SOL, our ground-based facility
- Scientific results
- Conclusion

3 – PICARD SOL, our ground-based facility (1/2)

Solar diameter telescope (SODISM-2)

Turbulence monitor

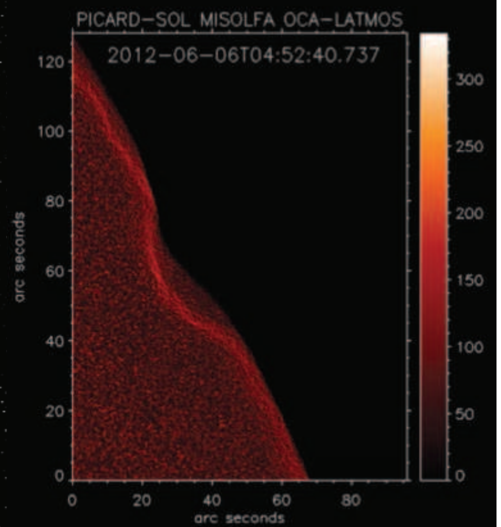

During the 2012 transit of Venus

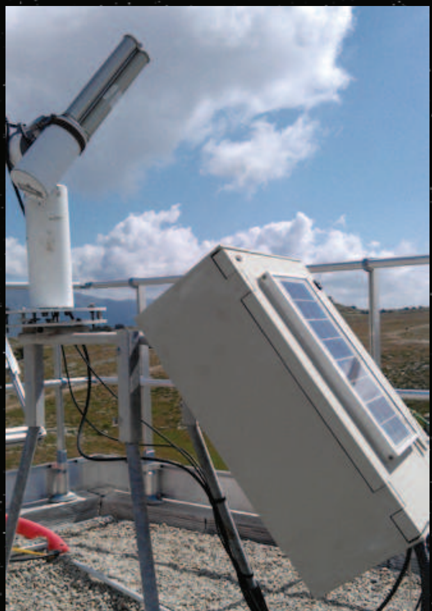

Photometer

Pyranometer

3 – PICARD SOL, our ground-based facility (2/2)


SODISM-2

Presentation outline

- The PICARD mission and the scientific objectives
- The PICARD/SODISM space instrument
- PICARD SOL, our ground-based facility
- Scientific results
- Conclusion

Solar Astrometry

Measure the diameter of the Sun (absolute value)

With PICARD/SODISM space instrument

4 – Scientific results

Solar radius determination is one of the oldest problems in astrophysics.
The transit of Venus on June 2012 provided a unique opportunity to determine the absolute radius of the Sun using solar imagers. The transit was observed from space by the PICARD spacecraft.

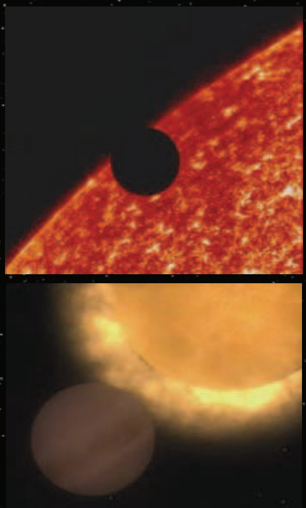

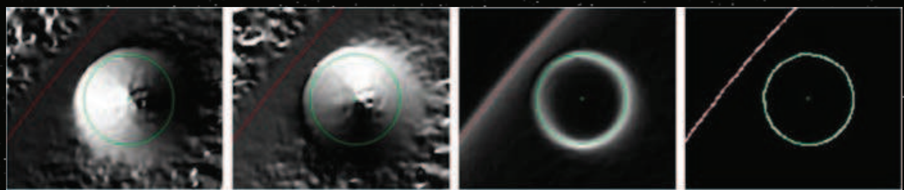

Meftah, Hauchecorne, Irbah et al., Sol. Physics, 2014

959.86 +/- 0.20 arc-seconds
Method: location of the inflection point

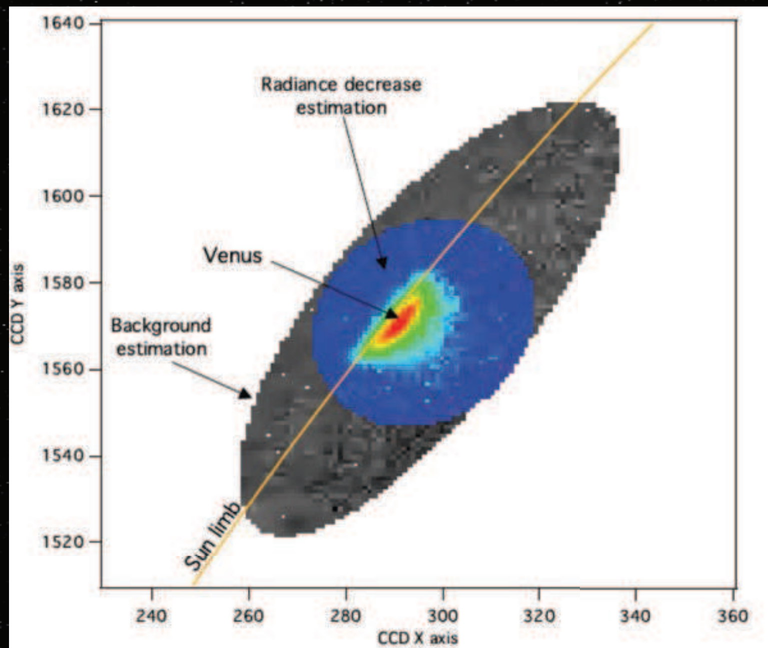

Hauchecorne, Meftah, Irbah et al., APJ, 2014

959.85 +/- 0.19 arc-seconds
Method: estimation of the decrease in the intensity (independent of the psf)

4 – Scientific results

Method for determining the radius of Venus and the Sun (IPP method)

- Noise removal (median filter to remove outlier pixels then a Gaussian blur is applied to smooth the edges in the image).
- Extracting contours (using a Sobel filter and the Canny method)

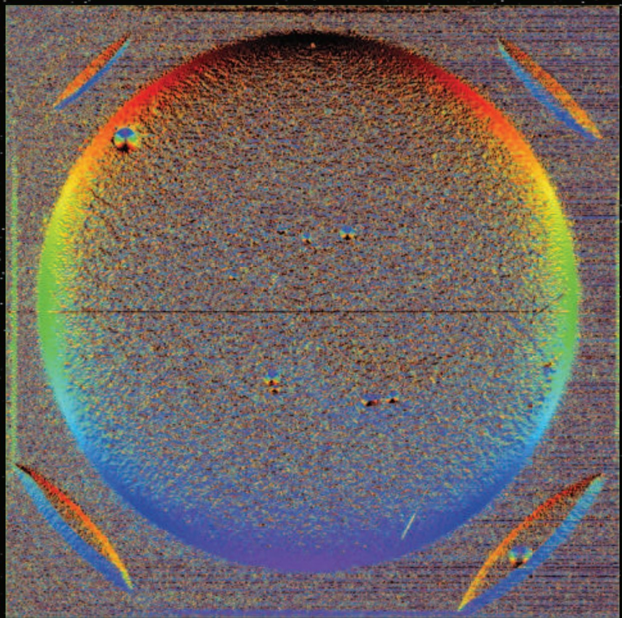

Horizontal gradient

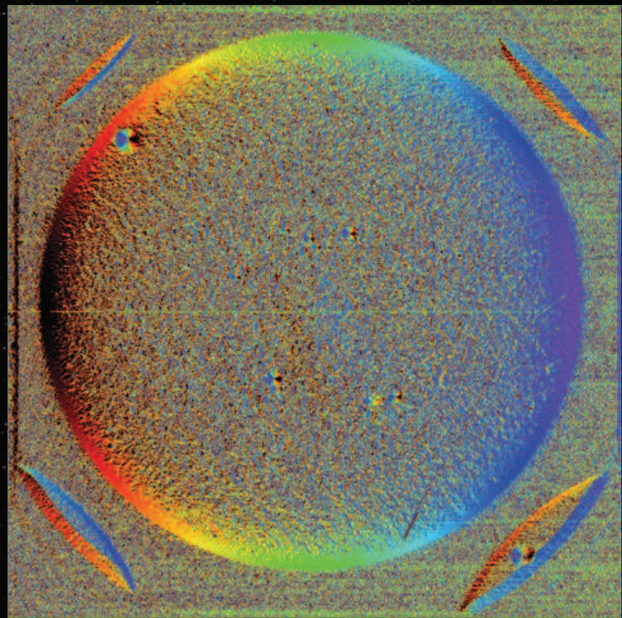

Vertical gradient

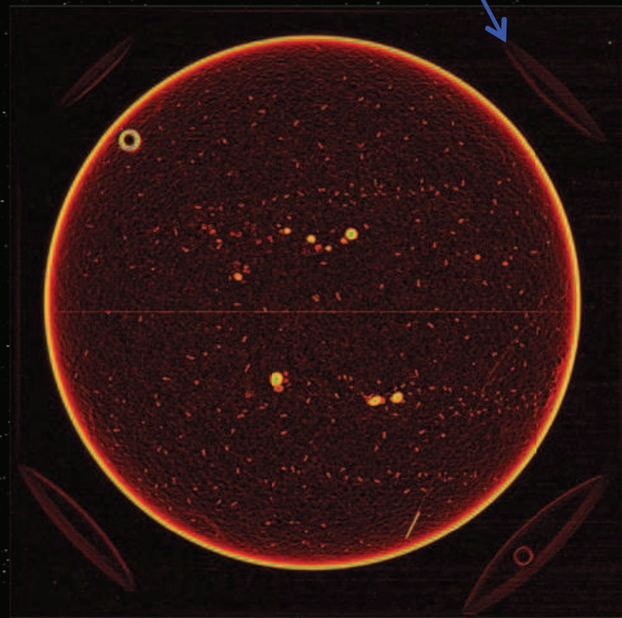

Norm of the gradient

4 – Scientific results

Method for determining the radius of Venus and the Sun (IPP method)

- Center detection using the Hough method
- Extracting the inflexion-point position (IPP)
- Characterizing the best fit (circle, ellipse, etc.)
- Determination of Venus radius and Sun radius

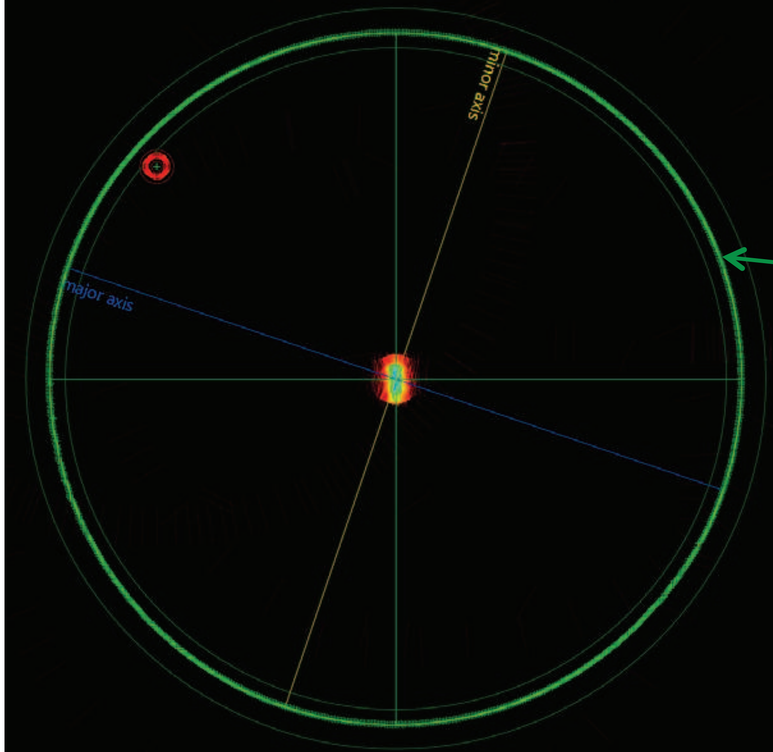

Venus and Sun “Hough” map

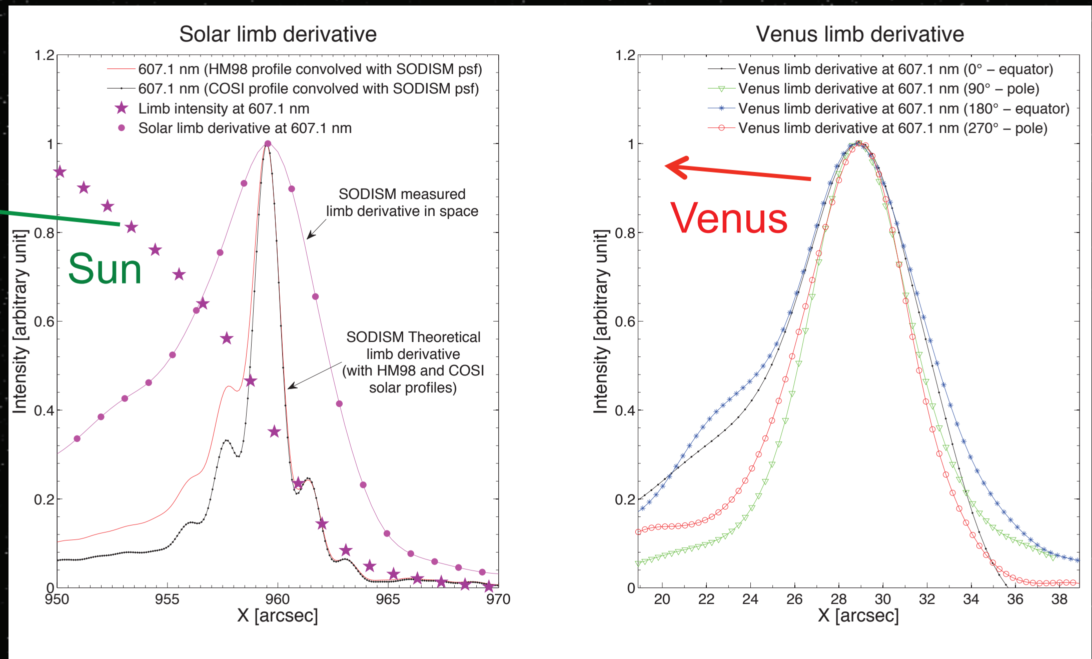

Extracting the inflexion-point position

4 – Scientific results

R = 696,156 ±145 km (PICARD)

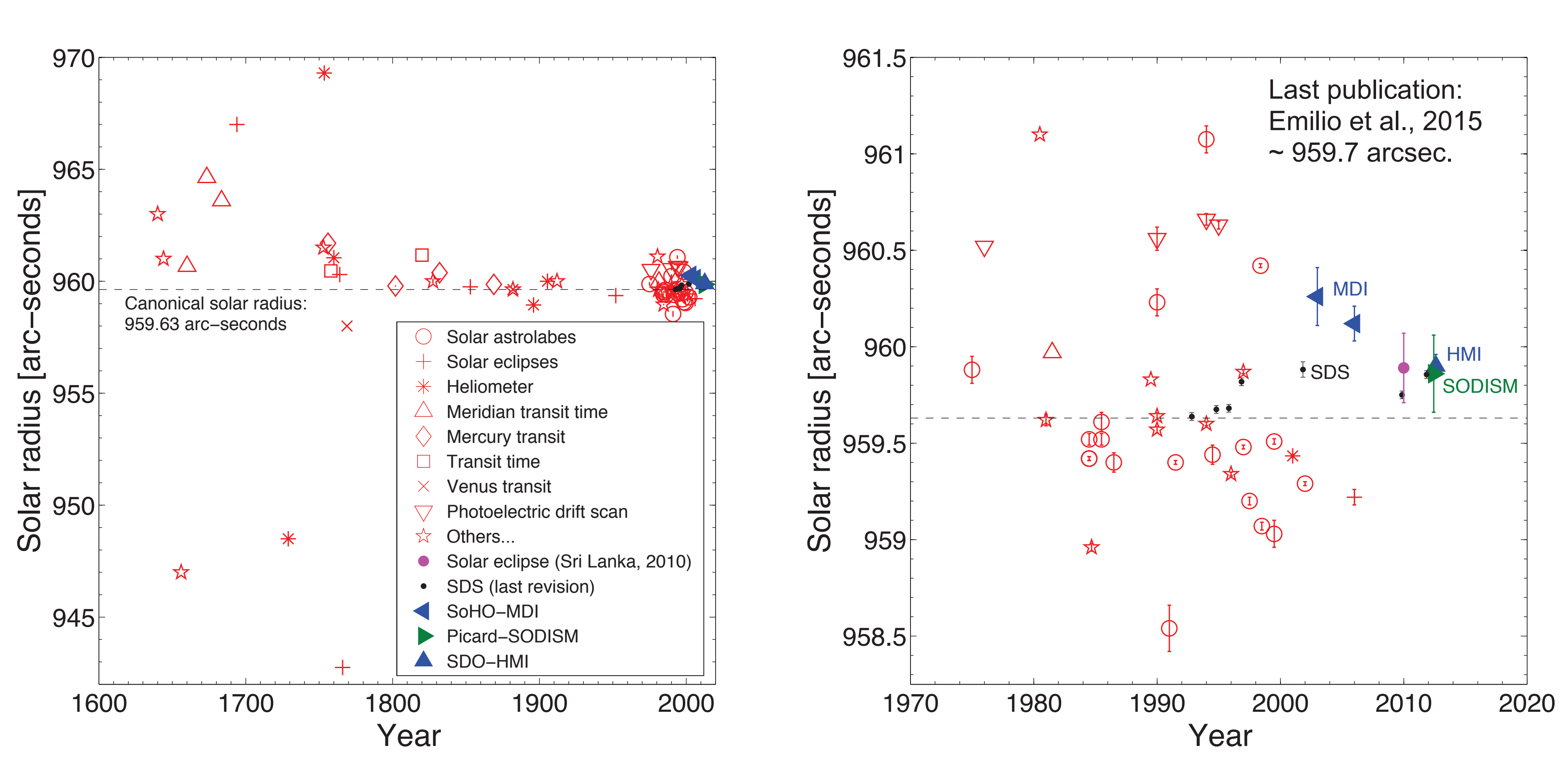

The work of the physicist is to establish a rigorous uncertainty budget.

Solar Astrometry

Measure the solar diameter variations over time

A) With PICARD ground-based facility
&
B) With PICARD/SODISM space instrument

4 – Scientific results

Measurements of the solar radius are of great interest within the scope of the debate on the role of the Sun in climate change.
Possible temporal variations of the solar radius are important as an indicator of internal energy storage and as a mechanism for changes in the TSI.

Space observations are a priori most favorable, however, space entails a harsh environment.
On ground, the instruments are affected by atmosphere.

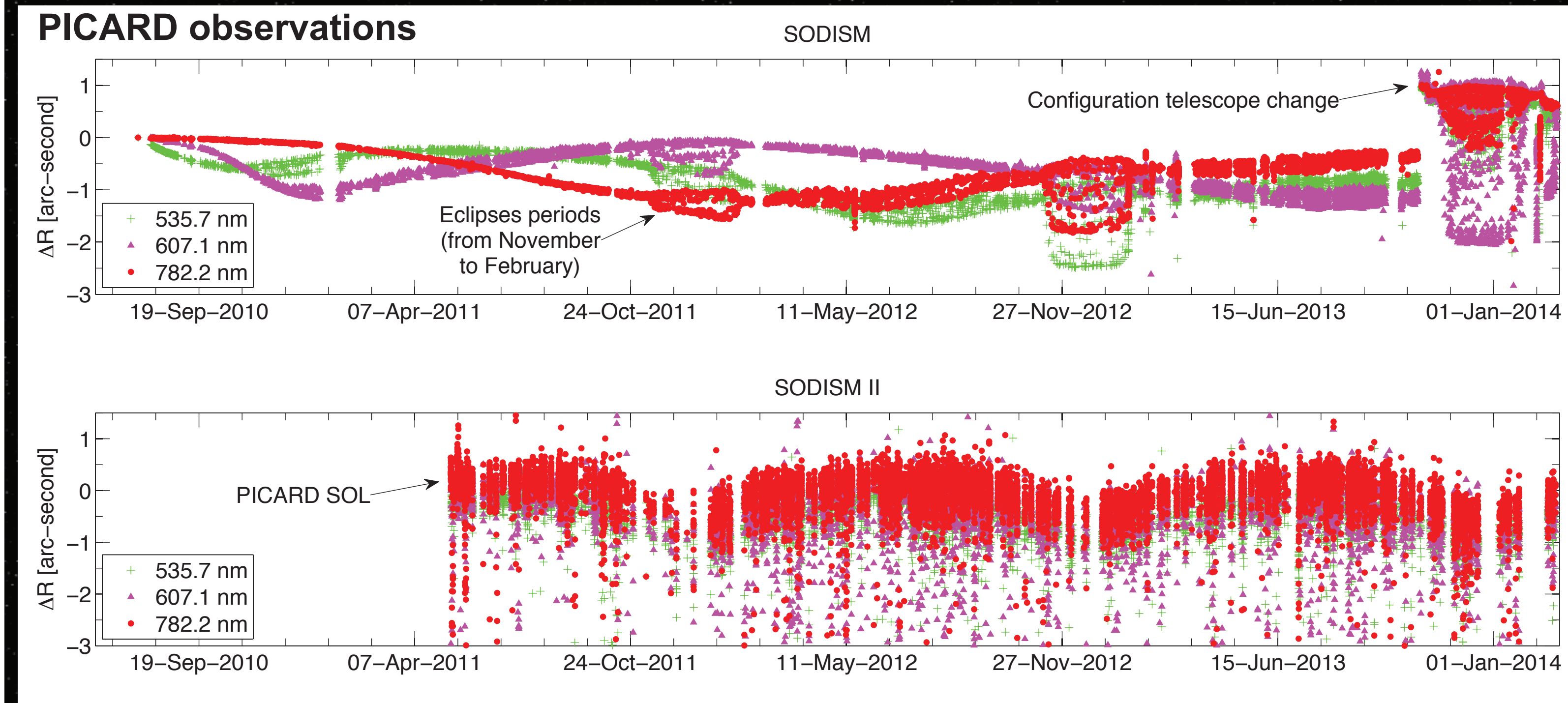

B) PICARD/
SODISM space instrument

A) PICARD
ground-based facility

4 – Scientific results

After corrections

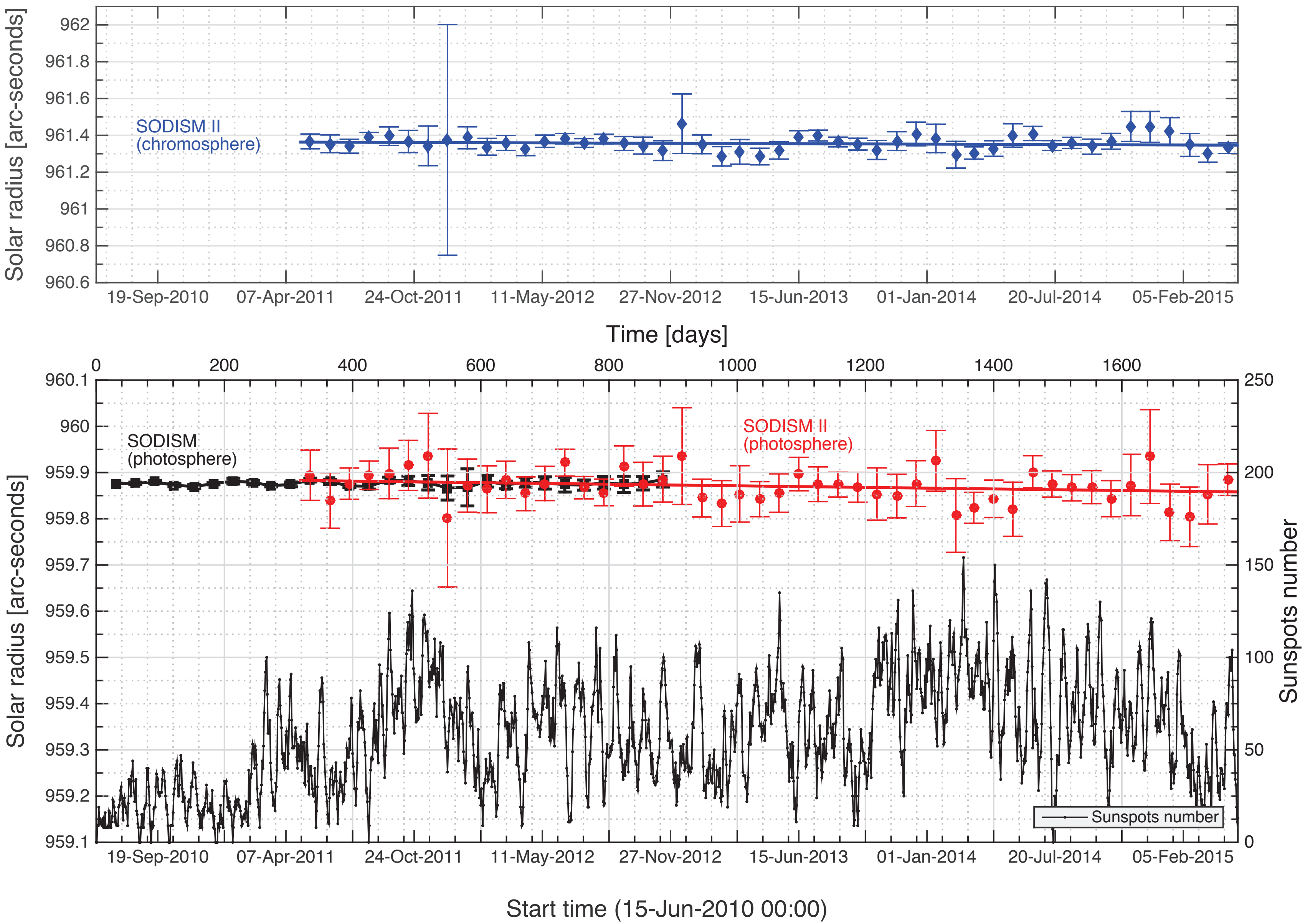

4 – Scientific results

A) PICARD ground-based facility corrections – Refraction and turbulence

Astronomical refraction (Ref) influences the solar radius measurements (more than 1 arc-seconds for observations made above 70° of zenith distance) that we obtain from images taken with SODISM II.

$$\mathrm{Ref} = \int_1^{n_{obs}} \tan\xi \frac{dn}{n} \quad (5a)$$

$$R_{cor} \simeq R_{obs} \times \left(C_{ref}(T_a, P_a, f_h, \lambda, z)\right)^{-1} \quad (5b)$$

$$C_{ref}(T_a, P_a, f_h, \lambda, z) = 1 - k(T_a, P_a, f_h, \lambda) \times \left(1 + 0.5 \times \tan^2(z)\right) \quad (5c)$$

$$k(T_a, P_a, f_h, \lambda) = \alpha_r(T_a, P_a, f_h, \lambda) \times \left(1 - \beta(T_a)\right). \quad (5d)$$

where $\alpha_r(T_a, P_a, f_h, \lambda)$ is the air refractivity for local atmospheric conditions at a given wavelength (Ciddor 1996), and $\beta(T_a)$ (see (Appendix B)) is the ratio between the height of the equivalent homogeneous atmosphere and the Earth radius of curvature at observer position assuming the ideal gas law for dry air (Ball 1908). In our calculation, we used a mean value of $k(T_a, P_a, f_h, \lambda)$.

$\alpha_r(T_a, P_a, f_h, \lambda)$ is the air refractivity for local atmospheric conditions at a given wavelength, and $n(T_a, P_a, f_h, \lambda)$ is the refractive index of air at the instrument (Ciddor 1996):

$$\alpha_r(T_a, P_a, f_h, \lambda) = n(T_a, P_a, f_h, \lambda) - 1. \quad (11)$$

$\beta(T_a)$ is the ratio between the height of the equivalent homogeneous atmosphere and the Earth radius of curvature at the observer position assuming the ideal gas law for dry air:

$$\beta(T_a) = \frac{P_a}{\rho \times g \times r_c} = \frac{C_a \times T_a}{r_c}, \quad (12)$$

where ρ is the air density, g is the gravity acceleration, C_a is a constant equal to 29.255 m K^{-1} (on the assumption that the ideal gas law is obeyed), and r_c represents the curvature of the Earth at Calern (~6,367,512 m).

Corrections are classics. Our ground results (PICARD SOL) were corrected for the effects of refraction and turbulence by numerical methods.

4 – Scientific results

The Figure shows the evolution of variations in solar radii observed at one AU by the two telescopes of the PICARD mission.

On the other hand, measurements carried out in orbit by SODISM show solar radius variations that are much greater than the expected order of magnitude (several milli-arc-seconds). The different measurements obtained from space show a temporal trend, which is wavelength dependent (this can be up to 3 arc-seconds on solar radius variations). For space data, the problem is complex.

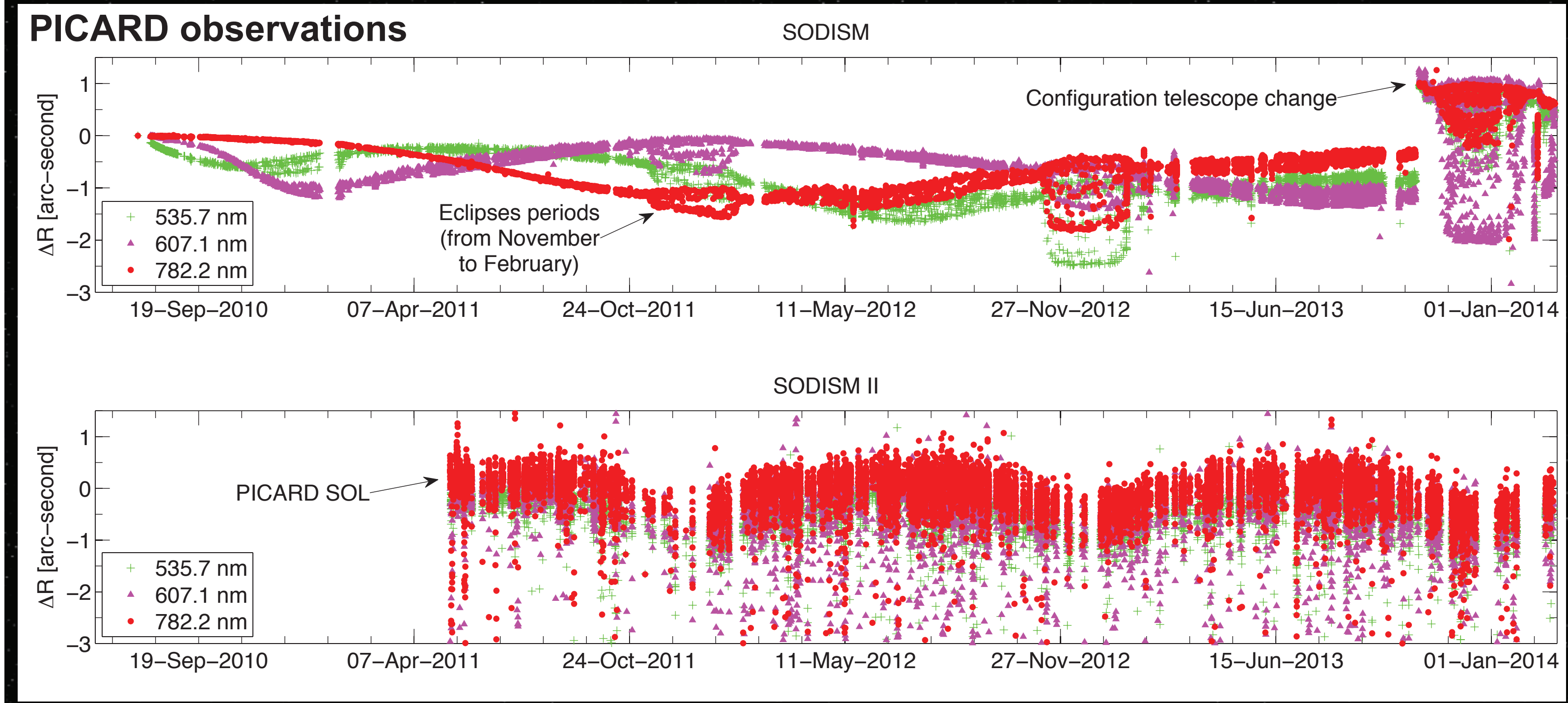

B) PICARD/ SODISM space instrument

A) PICARD ground-based facility

4 – Scientific results

B) PICARD SODISM space instrument solar radius variations and corrections

Several physical phenomena can lead to severe degradation of the optical performance of our space results (PICARD). In the case of SODISM, these effects entail solarization and polymerization of molecular contamination.

--- Normalized time series of integrated intensity during the PICARD space mission
→ High degradation in the UV

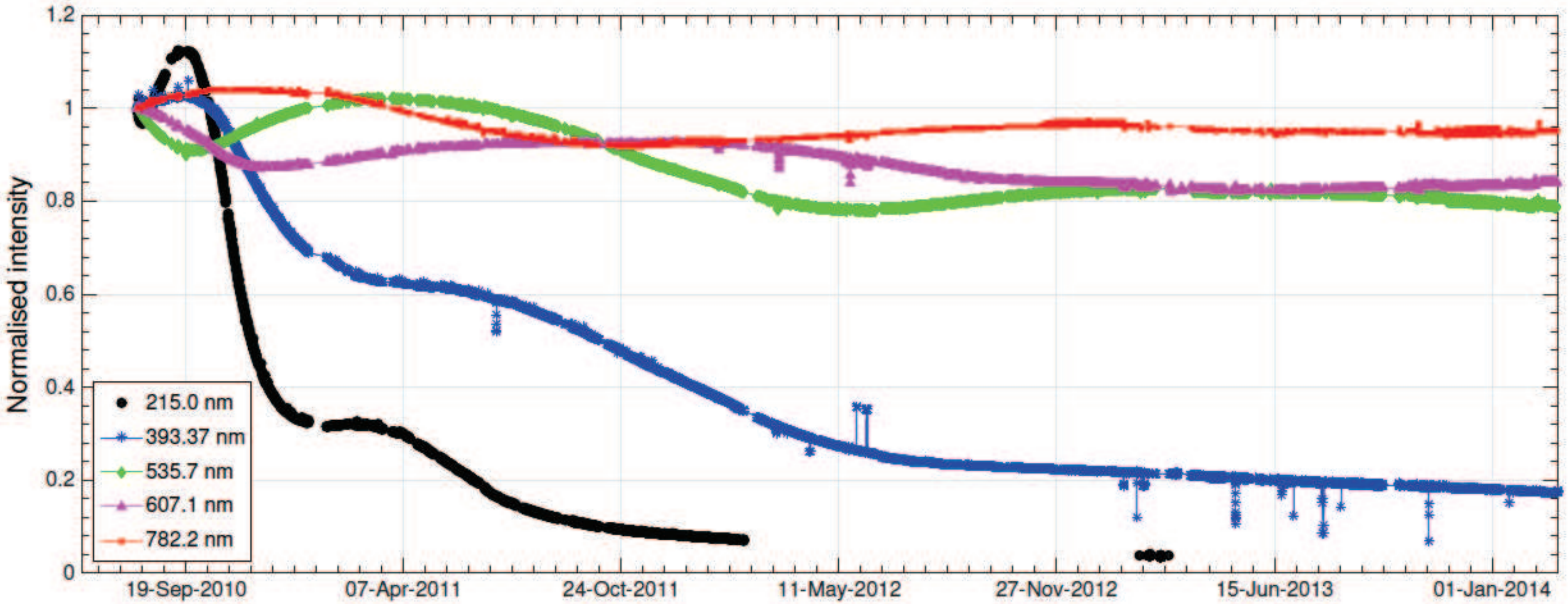

4 – Scientific results

B) PICARD SODISM space instrument solar radius variations

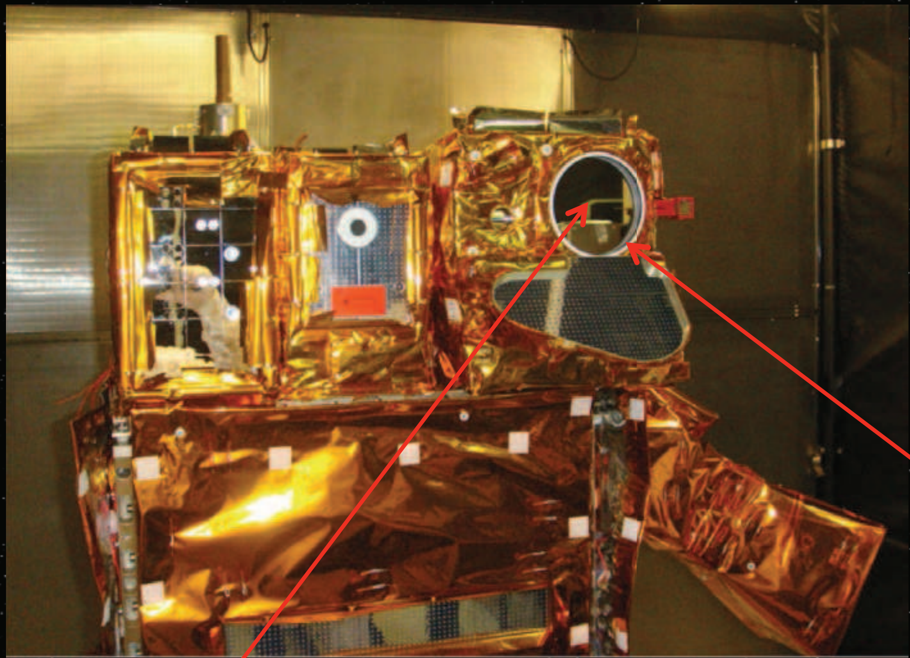

Two different solar absorption evolutions (optics, contour)

→ There is a very strong contamination of the satellite (due to solar panels, during the launch, etc.)

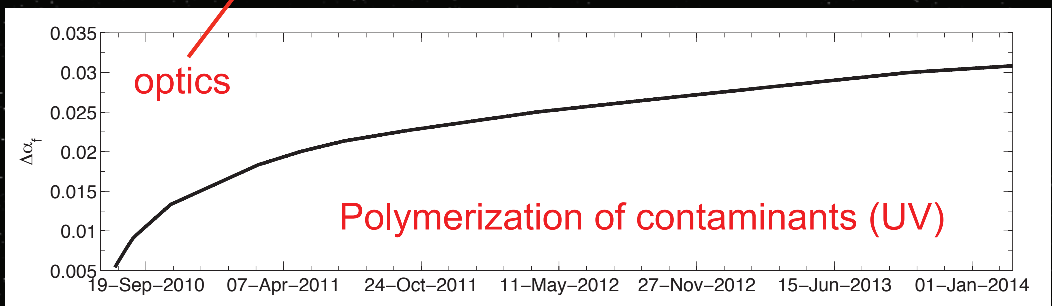

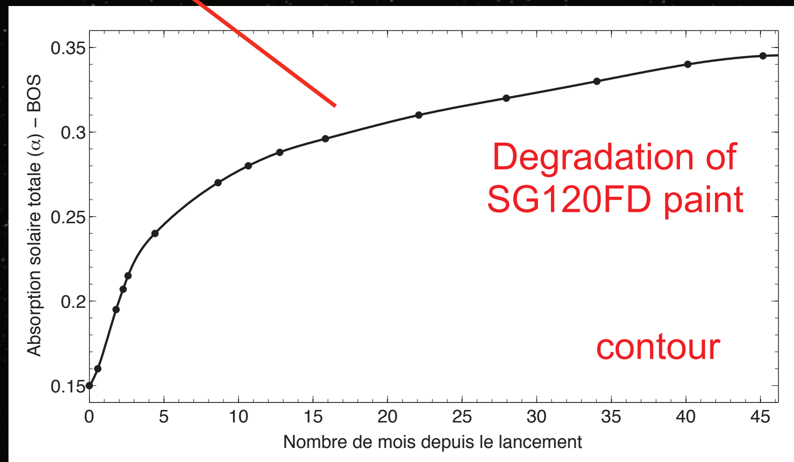

4 – Scientific results

B) PICARD SODISM space instrument measurements

--- Normalized time series evolution (contamination)

--- Important temperature change of SODISM front window and direct impact on solar radius measurements

→ How to correct the data?

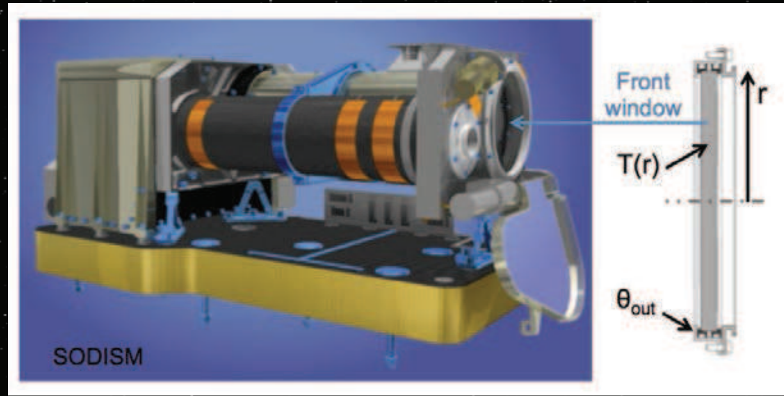

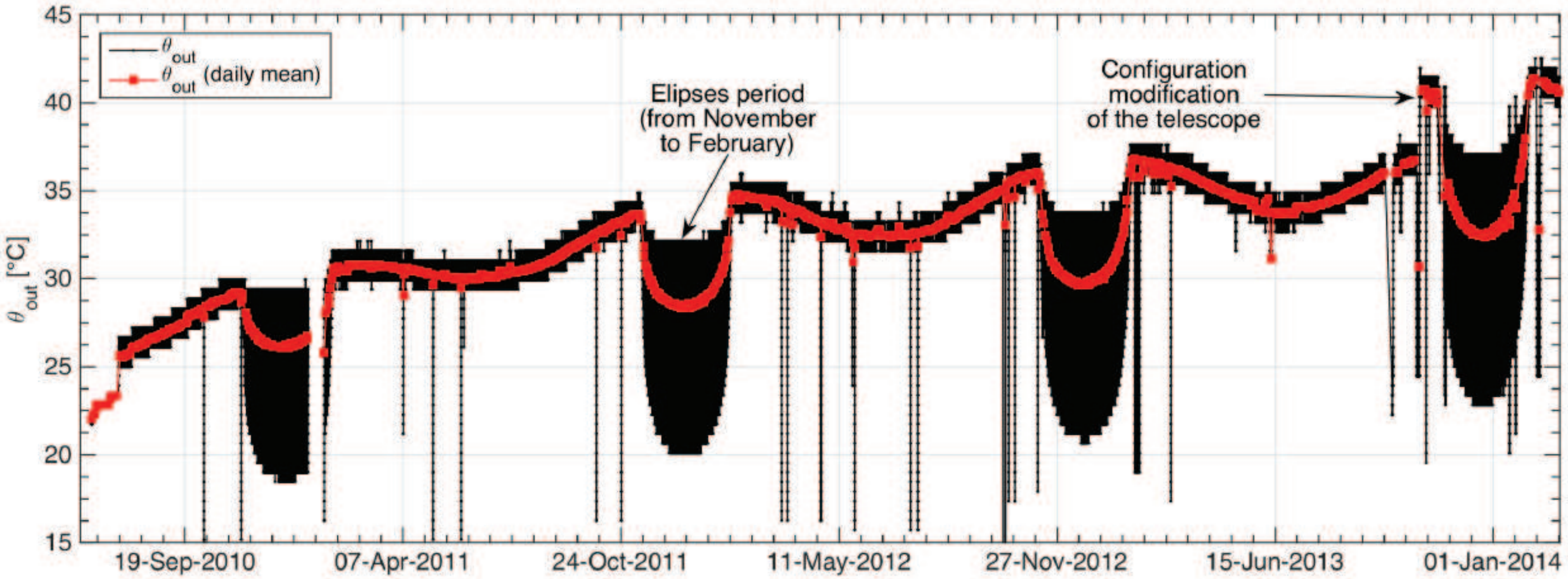

4 – Scientific results

LATMOS

B) PICARD SODISM space instrument measurements

We developed a simulator to try to correct the “signal” (thermo-optical effect).

Solar Spectrum (Atlas 3)
Solar flux (SOVAP, PREMOS, TIM, etc.)
IR and albedo flux (BOS)

SODISM intensities

Front window temperatures as function of housekeeping data

$$T = T_{\infty} + \frac{Flux}{\varepsilon_{out} \times \sigma \times \overline{\overline{T}}} + C_1 \times J_0(i \times r \times C) + C_2 \times Y_0(i \times r \times C)$$

Wave-front and Zenike polynomials

$$W_0 = \sum_{k=1}^{36} Z_k = f\left(\lambda, \frac{\partial n}{\partial T}, \Delta T(\alpha_f), \ldots\right)$$

Front window index vs. temperature

$$\frac{\partial n}{\partial T} = A_0 + A_1 \times \exp\left(\frac{-\lambda}{B_1}\right) + A_2 \times \exp\left(\frac{-\lambda}{B_2}\right)$$

$$E = \exp\left(2i \times \pi \times W_0\right)$$

Complex Wave-front

$$PSF_{SODISM} = \left(FFT2\left(E\right)\right)^2$$

PSF

Bi-dimensional fast Fourier transformer

$$LDF_{SODISM} = \left(\sum PSF_{SODISM}\right) * (LDF)$$

Limb darkening function → LDF_{SODISM}

Convolution

$$M_{False}(t) = FI_{SODISM}(t) * M_{True}(t)$$

Many instruments have this problem.

4 – Scientific results

B) PICARD SODISM space instrument measurements

Relation between solar radius and temperature gradient

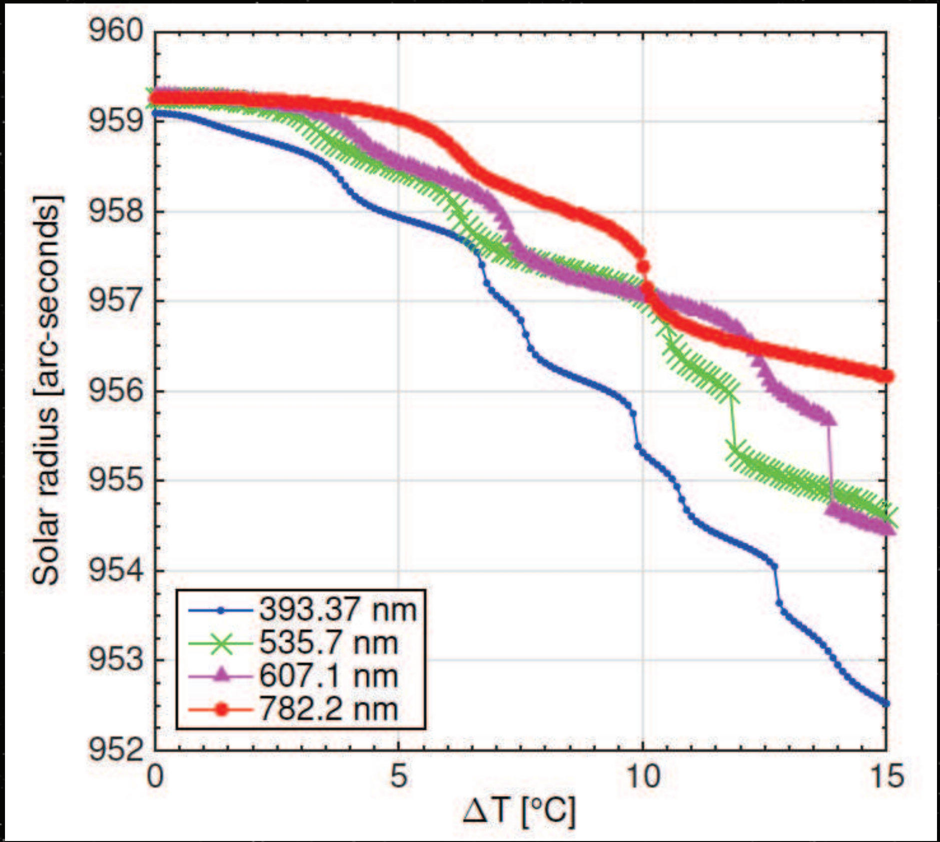

Evolution of the solar radius (determined by the inflection point method) as a function of a temperature gradient for different wavelengths.

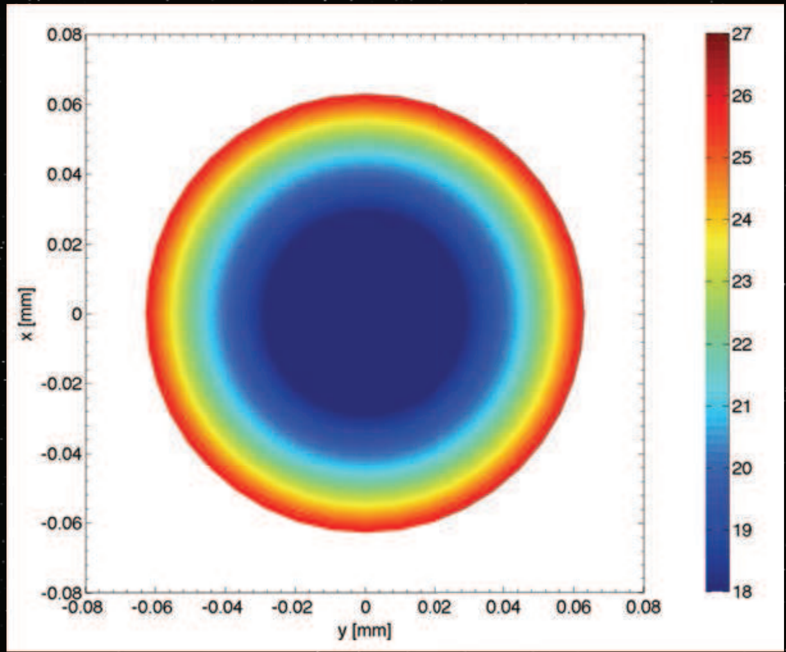

Temperature gradient on SODISM front window

4 – Scientific results

B) PICARD SODISM space instrument measurements

The space environment (UV effects, contamination, thermal cycling, etc.) combined with initial defects in telescope calibration (astigmatism, position of the focal plane, etc.) can degrade considerably the measurements taken by our instrument.

Solar models :
- COSI
- HM98
- Neckel2005

SODISM PSF is predominant

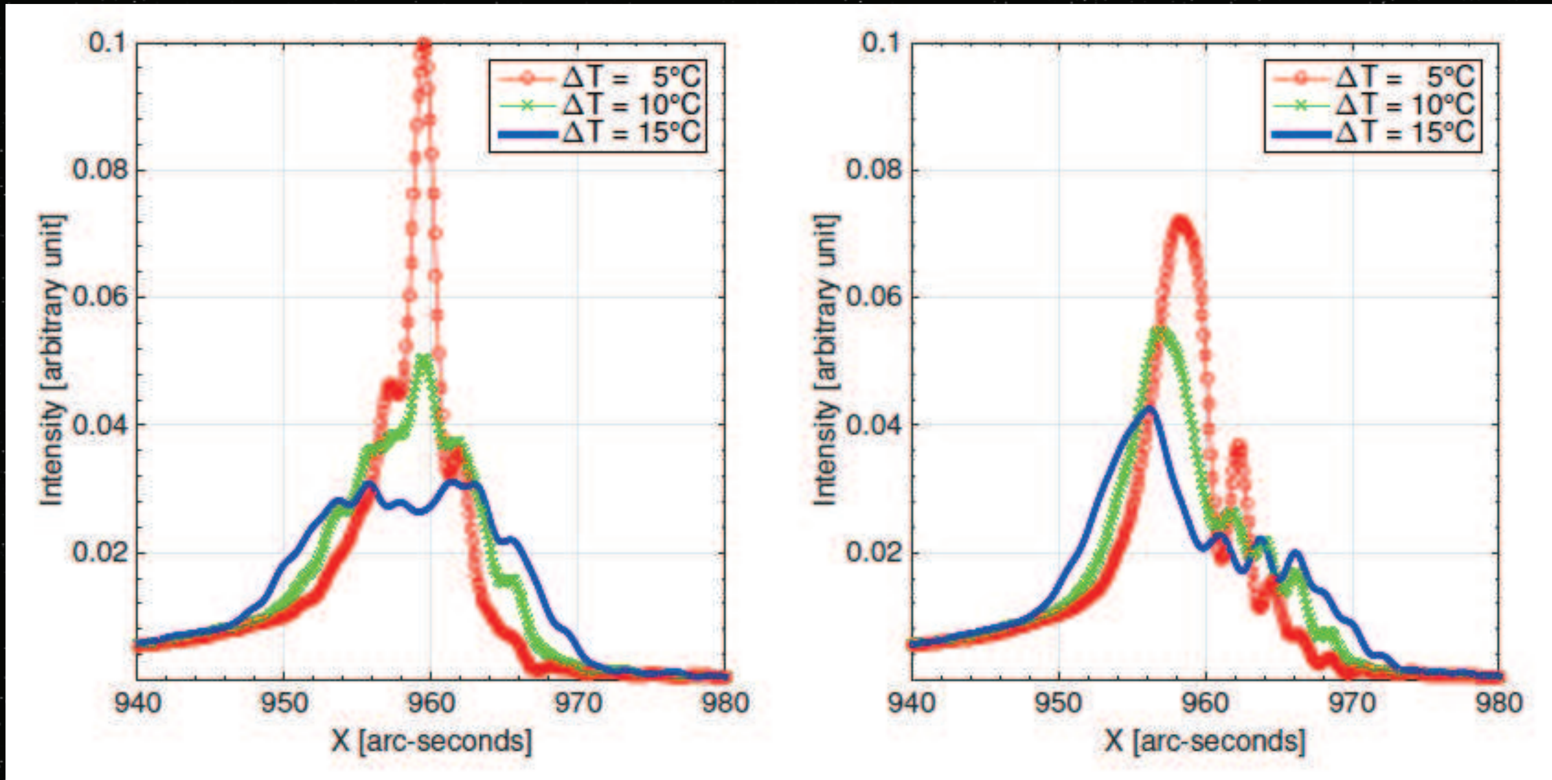

Evolution of the solar limb first derivative (simulation) for different angular sectors of the image. Consistent with what we observe.

4 – Scientific results

B) PICARD SODISM space instrument measurements

Temperature gradient evolution and uncertainty budget of the model

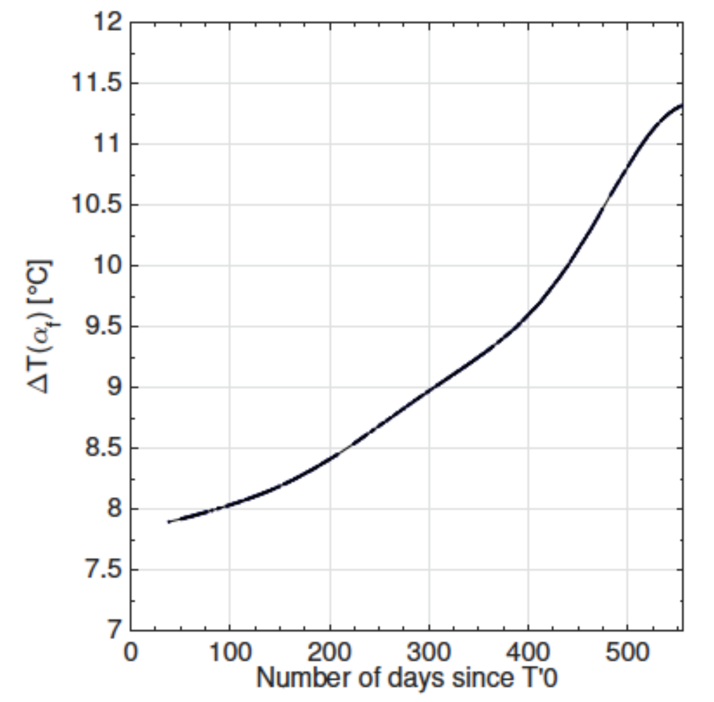

Evolution of the front window temperature gradient.

Uncertainty sources	Typical values	Uncertainty	Error on ΔT [°C]	Uncertainty type
$\alpha_f{}^{(a)}$	0.14	±0.001	±0.10	Test (S) & aging (R)
$\varepsilon_{out}{}^{(b)}$	0.81	±0.01	±0.30	Test (S)
$\Lambda^{(b)}$	1.38 W.m^{-1}.K^{-1}	±0.04 W.m^{-1}.K^{-1}	±0.31	Test (S)
$\theta_{out}{}^{(a)}$	22 °C	±0.10	±0.03	Calibration & measurement (S)
$\varphi_S{}^{(c)}$	1,362 W.m^{-2}	±2.4 W.m^{-2}	±0.02	Measurement (S)
$\varphi_{IR}{}^{(c)}$	238 W.m^{-2}	±6.0 W.m^{-2}	±0.02	Literature (S & R)
$\varphi_A{}^{(c)}$	~20 W.m^{-2}	±9.0 W.m^{-2}	±0.02	Literature (S & R)

Uncertainty budget.

- Spectral reflection and transmission measurements were performed with a spectrophotometer (Agilent Cary 5000 UV-NIS-NIR). The estimated tolerances are expected to be less than +/-1%.
- Near-normal IR reflectance measurements were performed in accordance with ASTM E408 (with an IR Reflectometer model DB100). The estimated tolerances are expected to be less than +/-1.5%.
- etc…

4 – Scientific results

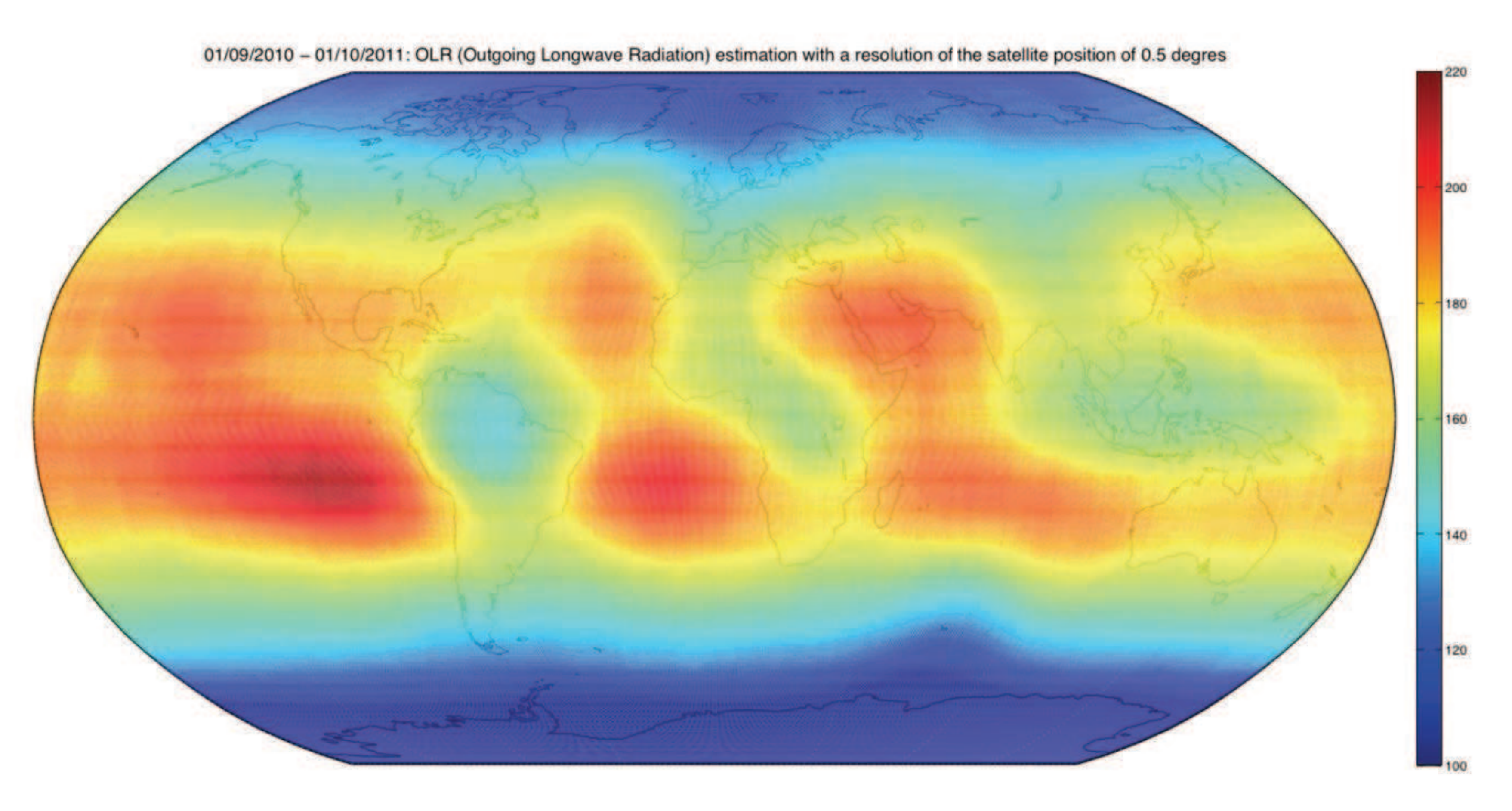

IR flux used in the model (obtained with PICARD data).

4 – Scientific results

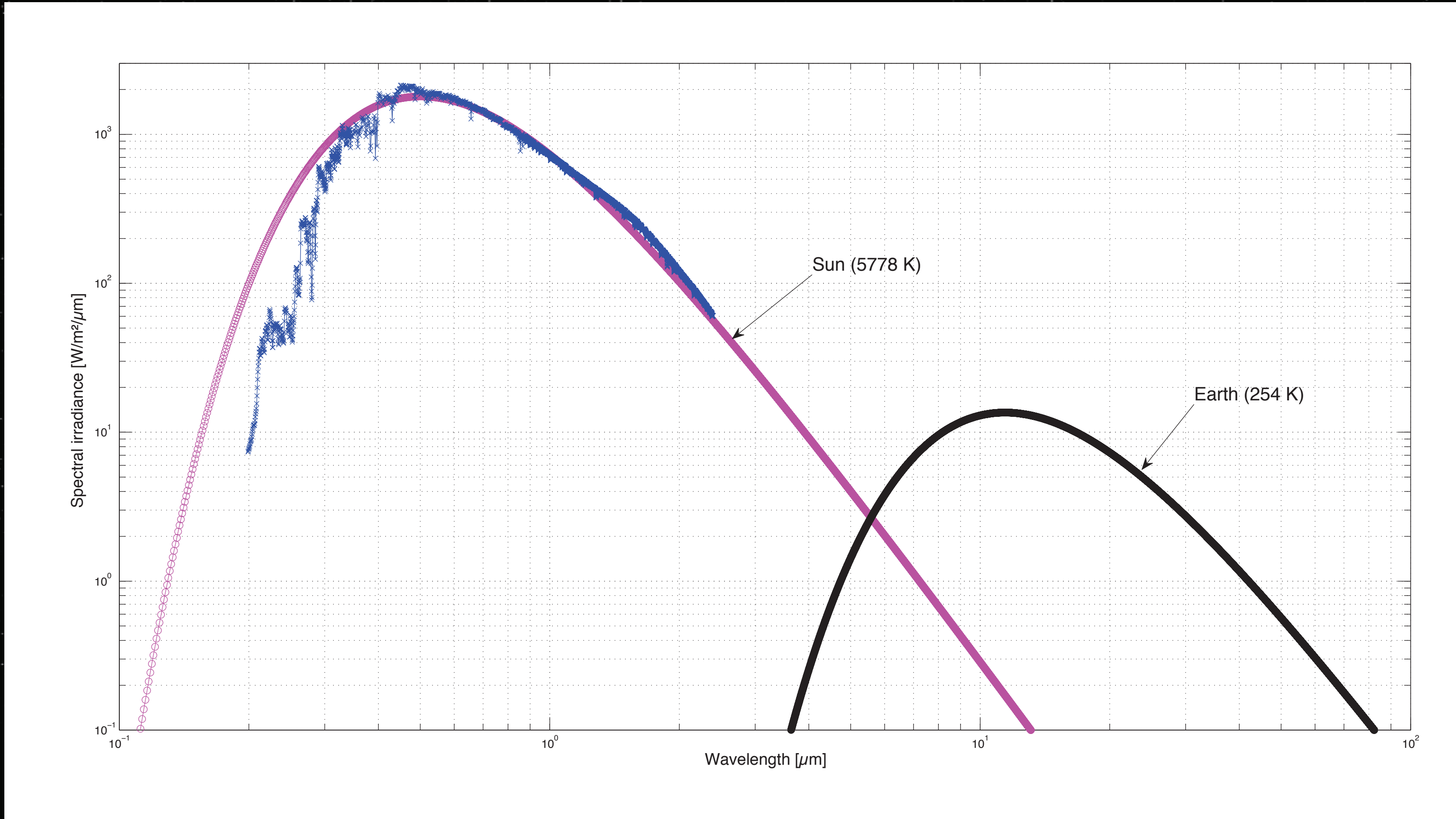

Solar spectrum used (ATLAS 3) in the model (obtained with PICARD data).

4 – Scientific results

Model equations:

$$T_{it+1}(r,t) = T_\infty + \frac{\text{Flux}(t)}{\varepsilon_{\text{out}} \times \sigma_b \times \overline{T(t)}} + C_1(t) \times J_0(i \times r \times C(t)) + C_2(t) \times Y_0(i \times r \times C(t)) \quad (3a)$$

$$\text{Flux}(t) = \alpha_f(t) \times \varphi_S(t) + \varepsilon_{\text{out}} \times fv_{ir}(t) \times \varphi_{\text{IR}}(t) + \alpha_f(t) \times fv_a(t) \times \varphi_A(t) \quad (3b)$$

$$\overline{T(t)} = (T_\infty + T_{it}(r,t)) \times \left(T_\infty^2 + T_{it}(r,t)^2\right) \quad (3c)$$

$$C(t) = \sqrt{\frac{\varepsilon_{\text{out}} \times \sigma_b \times \overline{T(t)}}{\Lambda \times h_w}} \quad (3d)$$

$$C_1(t) = \left(-\theta_{\text{out}}(t) \times Y_1(i \times r_c \times C(t))\right) / \left(J_1(i \times r_c \times C(t)) \times Y_0(i \times r_{\text{out}} \times C(t)) - J_0(i \times r_{\text{out}} \times C(t)) \times Y_1(i \times r_c \times C(t))\right) \quad (3e)$$

$$C_2(t) = \frac{-C_1(t) \times J_1(i \times r_c \times C(t))}{Y_1(i \times r_c \times C(t))}, \quad (3f)$$

Thermal model with Bessel functions

Optical model

$$w_0 = \sum_{k=1}^{36} C_k \times Z_k(\rho, \theta) \quad (1a)$$

$$C_3 = \frac{\delta \times D_{PS}^2}{16 \times \lambda \times f_S^2} + \frac{1}{2 \times \lambda} \times \frac{\partial n}{\partial T} \times h_w \times \Delta T(\alpha_f) \quad (1b)$$

$$\frac{\partial n}{\partial T} = A_0 + A_1 \times \exp\left|\frac{-\lambda}{B_1}\right| + A_2 \times \exp\left|\frac{-\lambda}{B_2}\right|, \quad (1c)$$

$$W(p_x, p_y) = A_{D_{PS}} \times e^{2i \times \pi \times w_0} \quad (2a)$$

$$\text{PSF}_{\text{SODISM}}(x,y) = \int_{-\infty}^{+\infty} \int_{-\infty}^{+\infty} W(p_x, p_y) \times e^{2i \times \pi \times (x \times p_x + y \times p_y)} \, dp_x \, dp_y \quad (2b)$$

$$\text{LDF}(r_S, \lambda) = \sqrt{1 - r_S^2}^{\,\alpha_S(\lambda)} \quad (2c)$$

$$\text{LDF}_{\text{SODISM}} = \int_{y_1}^{y_2} \text{PSF}_{\text{SODISM}}(x,y)\,dy \otimes \text{LDF}(r_S, \lambda). \quad (2d)$$

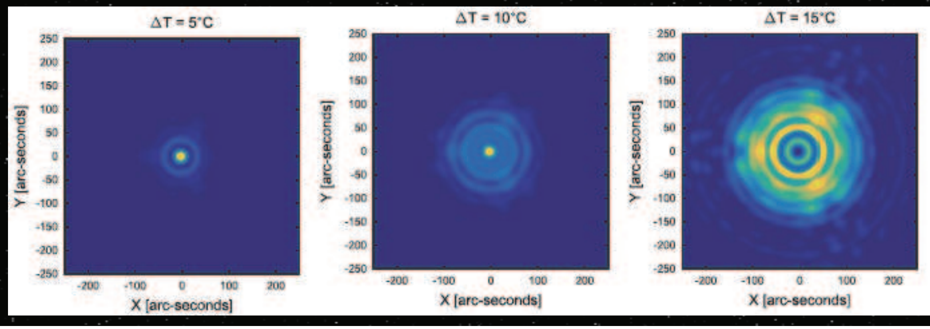

4 – Scientific results

B) PICARD SODISM space instrument measurements

Our space results (PICARD) were corrected for the temperature effects and contamination.

→ *$\Delta R_{\odot} < 20$ mas variations during the rising phase*

We find a small variation of the solar radius from space measurements with a typical periodicity (6.5 mas variation in the solar radius with a periodicity of 129.51 days → same with ground-based).

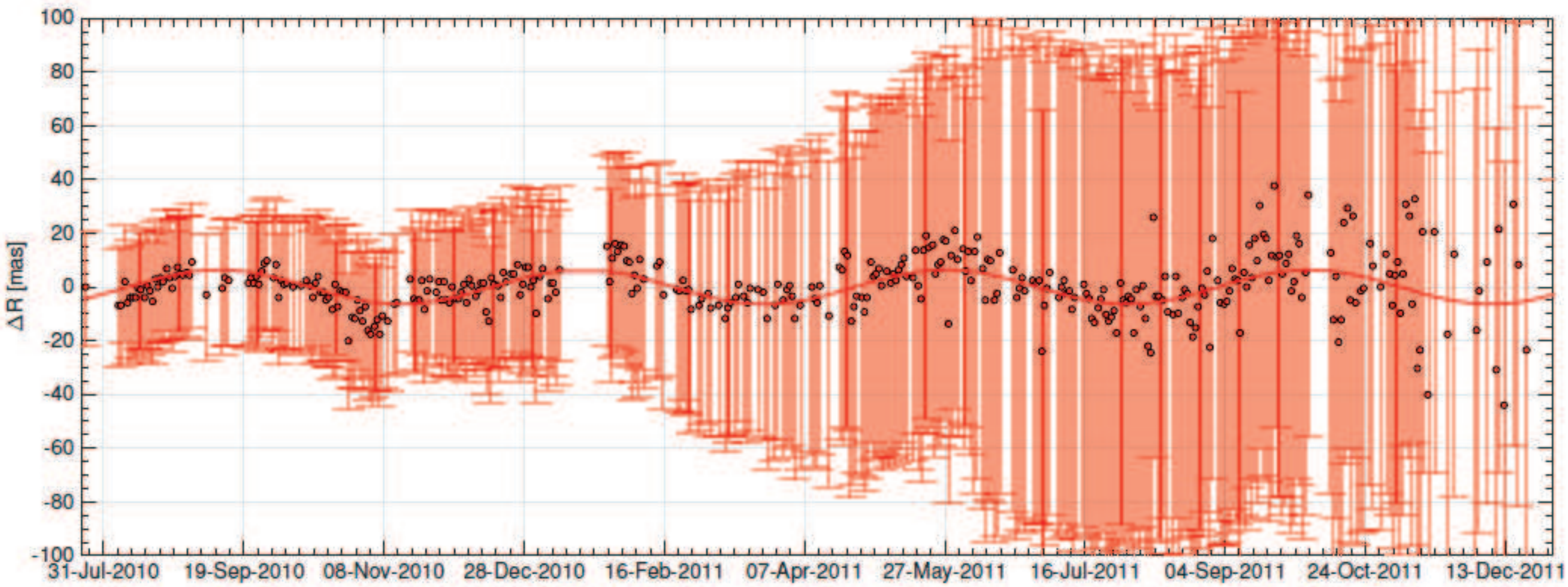

Meftah, Hauchecorne, Irbah et al., APJ (2015).

4 – Scientific results

B) PICARD SODISM space instrument measurements

For studies of our different time series data (solar radius), it is crucial to know at what time scales certain periodicities occur or recur.
In our application, we need to know the frequency and temporal information at the same time.
We use:

- Wavelet Analysis to Study Solar Radius (in particular Morlet Wavelet)

$$W(b,a) = \frac{1}{\sqrt{a}} \int \psi^* \left(\frac{t-b}{a}\right) f(t)dt$$

It is common to have incomplete or unevenly sampled time series for a given variable. Determining cycles in such series is not directly possible with methods such as Fast Fourier Transform (FFT) and may require some degree of interpolation to fill in gaps. An alternative is the Lomb-Scargle method.

$$P_N(w) = \frac{1}{2\sigma^2}\left(\frac{\left(\sum_{k=1}^{N}(x_k-\bar{x})\cos(w(t_k-\tau))\right)^2}{\sum_{k=1}^{N}\cos^2(w(t_k-\tau))} + \frac{\left(\sum_{k=1}^{N}(x_k-\bar{x})\sin(w(t_k-\tau))\right)^2}{\sum_{k=1}^{N}\sin^2(w(t_k-\tau))}\right)$$

4 – Scientific results

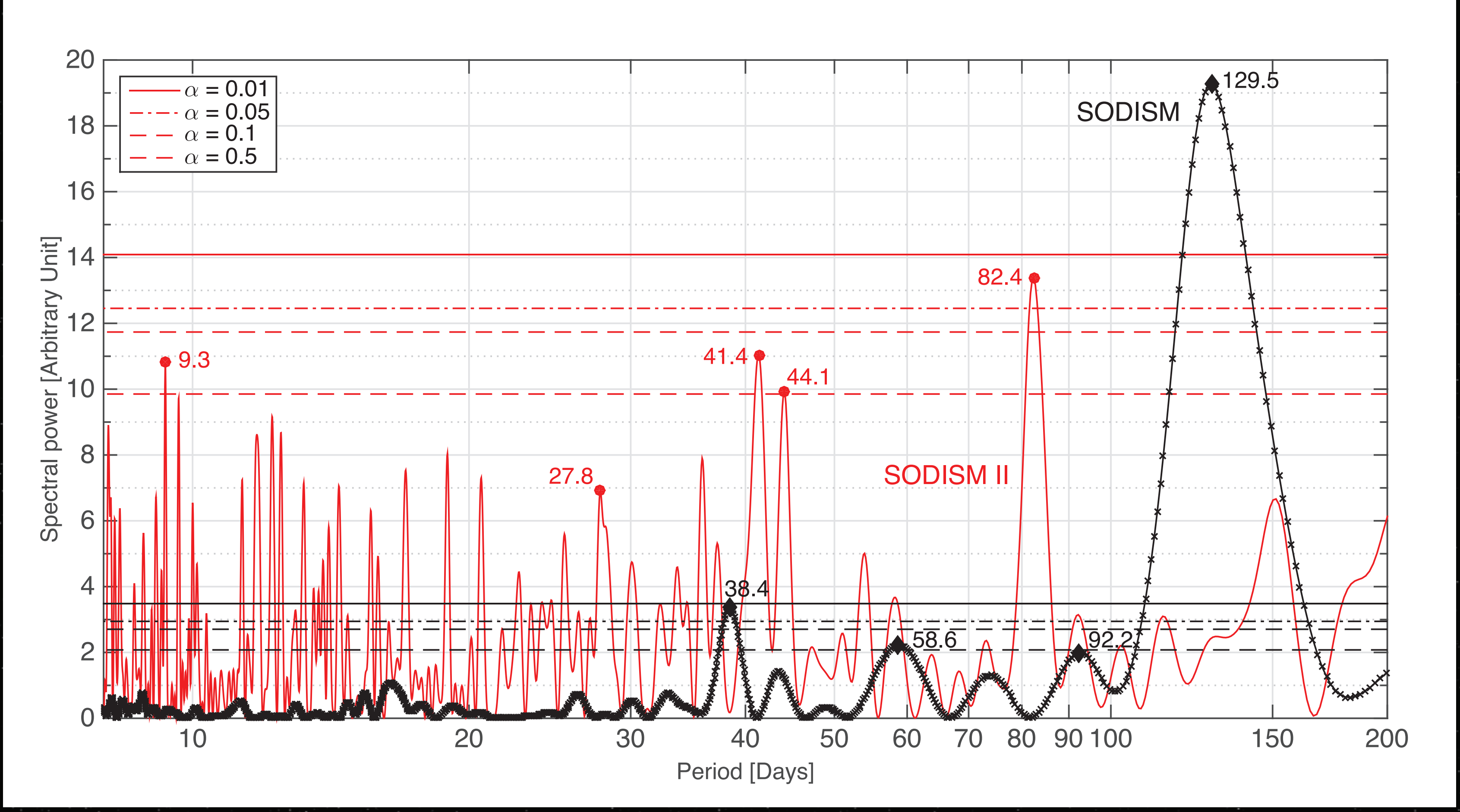

Solar radius Lomb-Scargles periodogram (all the data)

4 – Scientific results

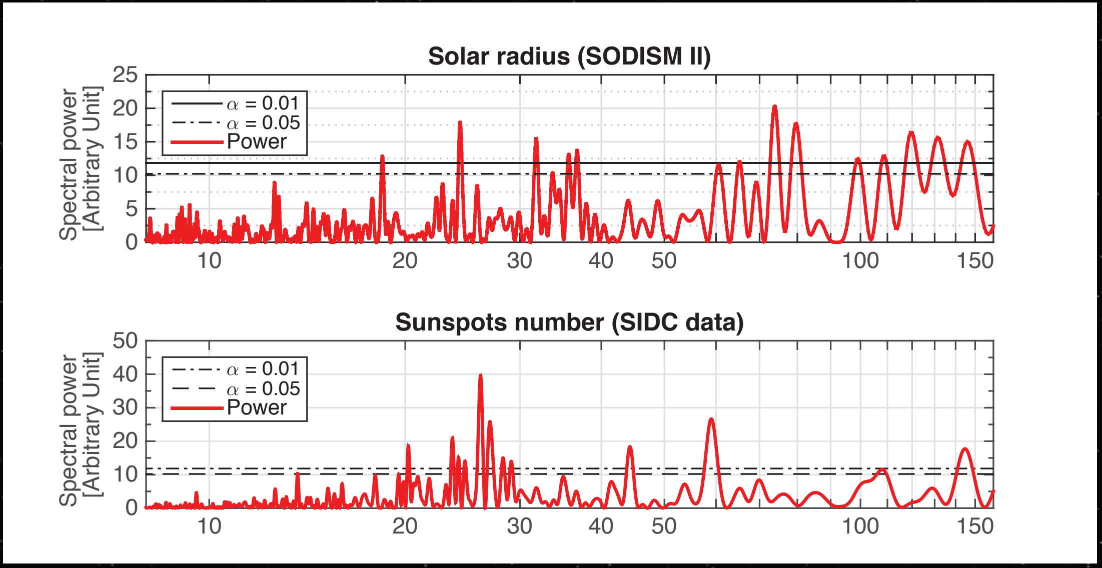

Solar radius Lomb-Scargles periodogram (daily mean) → better approach

→ *$\Delta R_{\odot} < 20$ mas variations*

Table 1. Solar radius periodicities with statistical significance level of over 99%. Long periodicities (greater than 300 days) are not resolved due to *Picard* short periods of observation.

Instrument	Period [days]	Variations [mas rms]
PICARD-SODISM	129.5	4.6
(Jul. 2010-Jan. 2012)	–	–
PICARD-SODISM II	18.4	14.5
(May 2011-May 2015)	24.3	16.2
	31.8	14.2
	35.6	12.0
	36.7	12.5
	65.1	11.5
	74.0	14.8
	79.5	14.9
	99.3	11.8
	108.4	11.1
	119.4	13.5
	131.4	13.4
	146.0	12.9

This finding sheds new light on the solar dynamo mechanism, where very small solar radius variations (0.02 arc-second root mean square) are linked with magnetic activity for typical solar periodicities (130-days (Bai, 2003) and 154-days (Rieger period)). Periodicities in Solar Flare Occurrence (130-days) link.

4 – Scientific results

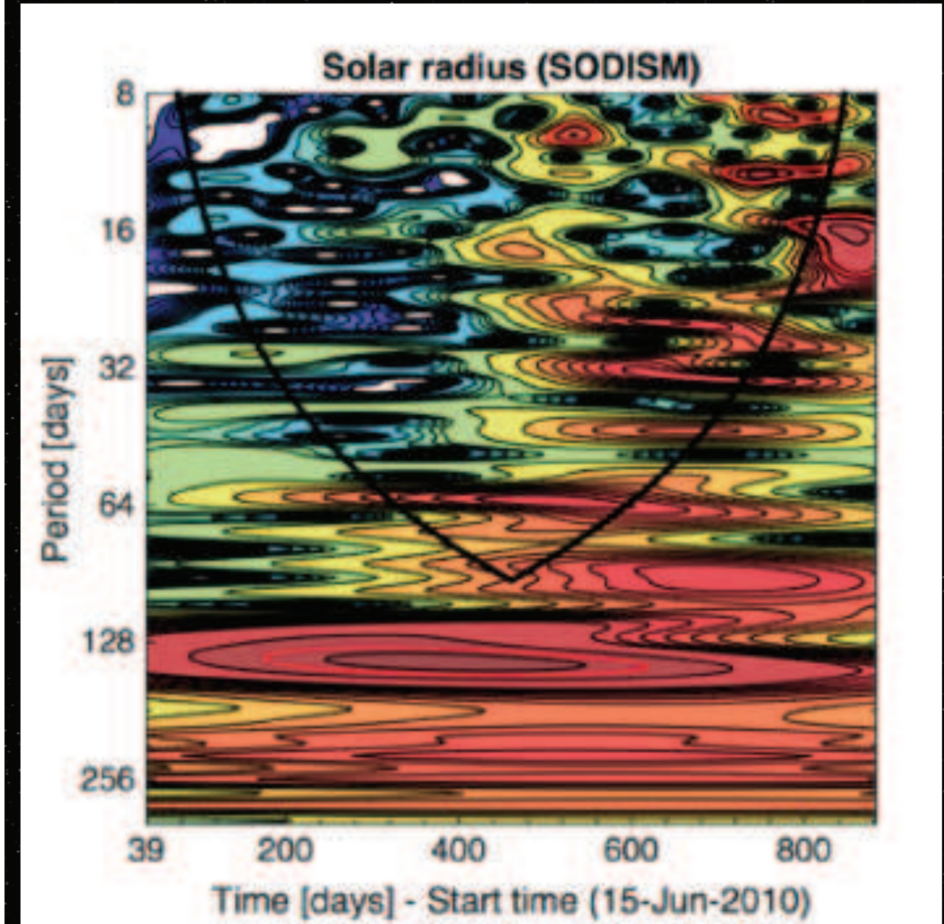

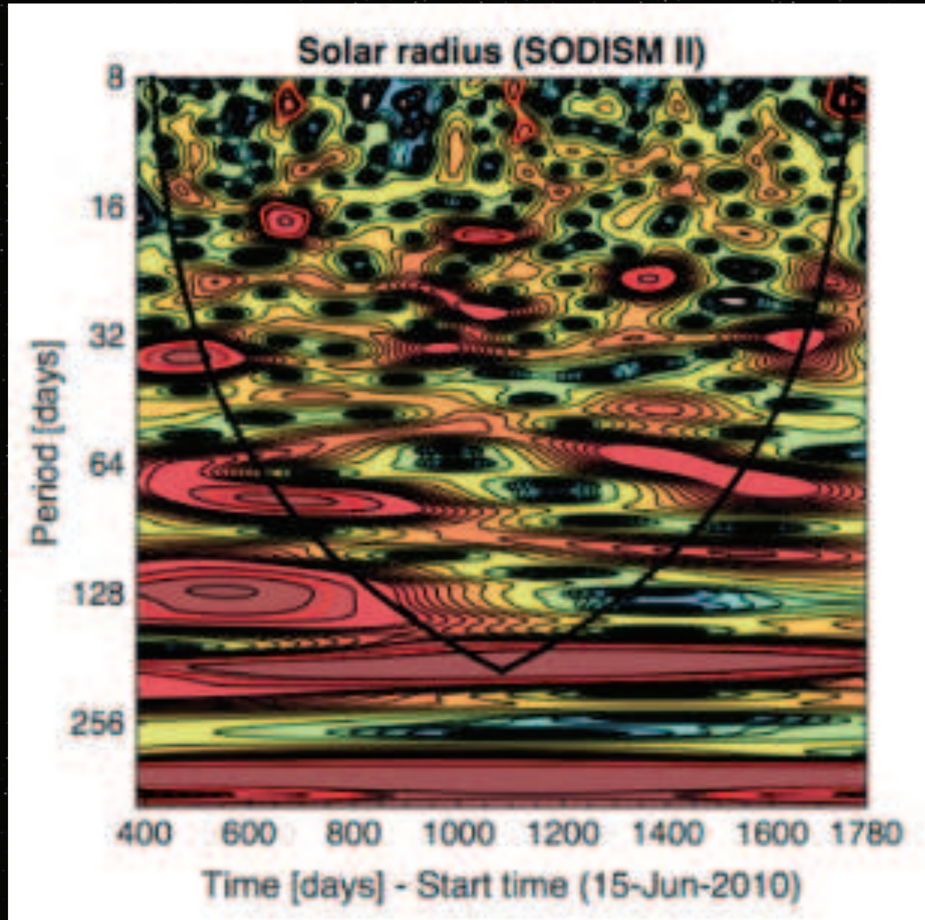

4 – Scientific results

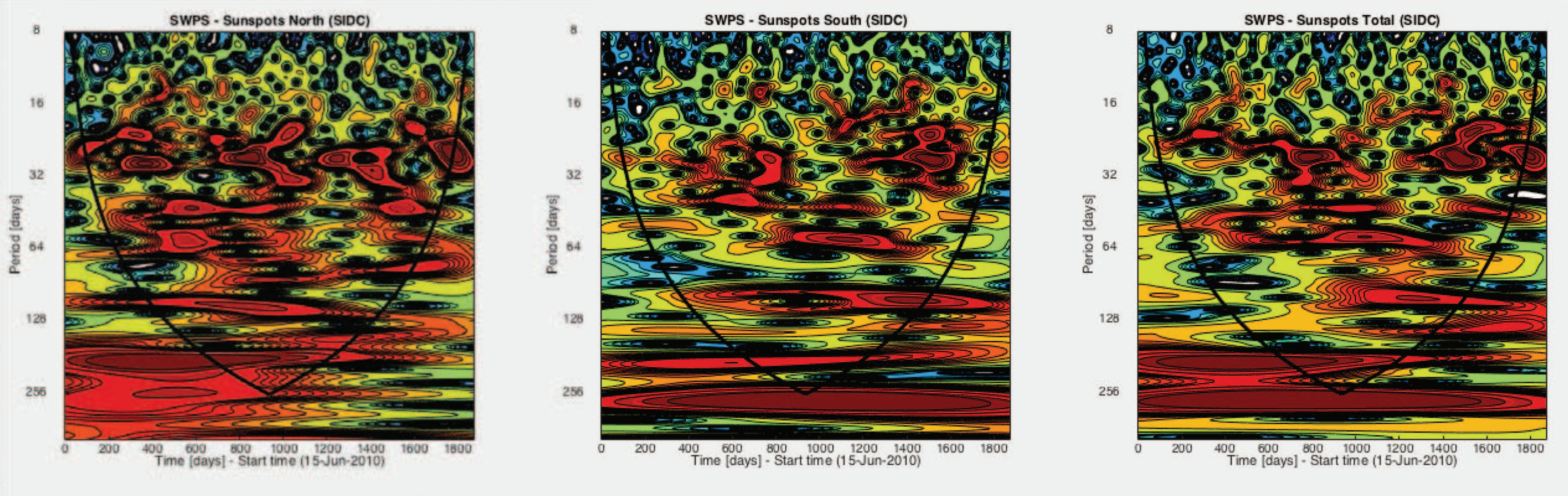

DAILY SUNSPOT AREA AVERAGED OVER INDIVIDUAL SOLAR ROTATIONS

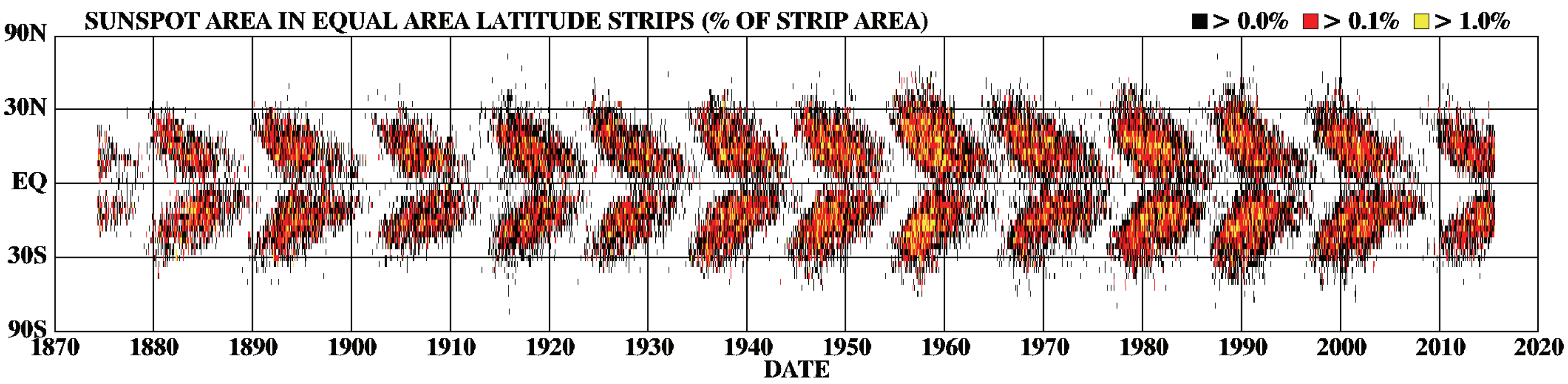

4 – Scientific results